



Uncertainty Analysis Related to Beach Morphology and Storm Duration for More Reliable Early Warning Systems for Coastal Hazards

J. L. Garzon¹ , T. A. Plomaritis² , and Ó. Ferreira¹

¹CIMA—Centre for Marine and Environmental Research, FCT, Universidade do Algarve—Campus de Gambelas, Faro, Portugal, ²Department of Applied Physics, Faculty of Marine and Environmental Science, University of Cadiz—Campus Rio San Pedro (CASEM), Cadiz, Spain

Key Points:

- In steep sites, pre-storm profile variability induces high uncertainties in berm retreat for medium events and dune retreat for large events
- Variations in storm duration cause high dune erosion uncertainties for large events, especially for beach morphologies with less sediment
- Prediction systems must consider the variability of beach morphology and storm duration for accurate forecasts, especially in steep beaches

Supporting Information:

Supporting Information may be found in the online version of this article.

Correspondence to:

J. L. Garzon,
jlhervas@ualg.pt

Citation:

Garzon, J. L., Plomaritis, T. A., & Ferreira, Ó. (2023). Uncertainty analysis related to beach morphology and storm duration for more reliable early warning systems for coastal hazards. *Journal of Geophysical Research: Oceans*, 128, e2022JC019339. <https://doi.org/10.1029/2022JC019339>

Received 30 SEP 2022
Accepted 12 MAY 2023
Corrected 3 JUN 2023

This article was corrected on 3 JUN 2023.
See the end of the full text for details.

Abstract Early warning systems (EWSs) for coastal erosion are cost-effective instruments for risk reduction. Among other aspects, the selection of the pre-storm beach morphology and the definition of storm characteristics can affect EWS reliability. Here, XBeach simulations were used to assess the uncertainties in beach-dune erosion related to the variability of storm severity and duration and pre-storm morphology. Wave height return periods (from 5 to 50 years) determined the severity and the duration variability was established from confidence intervals after an adjustment with wave height. The variability of steep profiles included different berm morphologies (from fully developed to eroded berms). Three indicators, relative eroded volume, proportional berm retreat and proportional dune retreat, were evaluated. The experiments revealed that: (a) Relative eroded volume uncertainties related to the pre-storm morphology variability were slightly lower (maximum 8%) than the uncertainties related to storm duration (11%–18%). (b) Pre-storm profile variability can induce large uncertainties in the proportional berm retreat (up to 88%) for moderate events such as the 5- and 10-year events. Storm duration variability had less influence on this indicator (maximum 12%). (c) The uncertainties in the proportional dune retreat increased with storm severity and they ranged between 14% and 41% for pre-storm profile variability and between 2% and 40% for storm duration variability. Duration variability even governed the occurrence of dune breaching on eroded berm profiles in the most extreme event. Hence, the uncertainties related to initial/forcing conditions, namely pre-storm morphology and storm duration, must be assessed to develop reliable coastal erosion EWSs.

Plain Language Summary Large sea storms generate high waves that can erode or remove sand from the coast, damaging recreational infrastructures and even building foundations. Under these dramatic situations, early warning systems (EWSs) are helpful instruments to alert communities about the risks of incoming storms. EWSs normally use computational models to calculate sand removal based on the shape of the beach before the arrival of the storm (so-called pre-storm profile) and storm characteristics. The pre-storm profile is not fixed but evolves along the year as the response to the incoming waves. However, updated measurements of the pre-storm profile are not always available. Regarding the storm characteristics affecting coastal erosion, we investigated the importance of the period of time in which high waves are reaching the beach (so-called storm duration). The computational model results display that the pre-storm profile used by this model must be close to reality to obtain reliable predictions of the beach and dune erosion. Similarly, storm duration is very important to produce accurate beach and dune change predictions and it should be also considered in the model. This research highlights the importance of knowing the pre-storm profile and storm duration to develop EWSs that provide reliable predictions to reduce damages in coastal communities.

1. Introduction

Many coastal zones are heavily populated and they host highly valuable socioeconomic activities (e.g., recreation and tourism). Among the different coastline typologies, sandy beaches and dunes occupy 30% of the global coastline (Luijendijk et al., 2018). These features represent the interface between land and ocean and protect many coastal communities against flooding and erosion. However, an important portion of these sandy environments is currently suffering from long-term structural erosion or landwards shoreline migration (Mentaschi et al., 2018). On a shorter temporal scale, beaches can be subject to the impact of severe coastal storms that may induce catastrophic morphological changes and compromise the protected urbanized areas. Some examples of

the recent storms responsible for devastating erosive episodes are Hurricane Sandy 2012 (Smallegan et al., 2016), Storm Hercules 2014 (Castelle et al., 2015), Storm June 2016 (Harley et al., 2017), Storm Emma 2018 (Ferreira et al., 2019), and Storm Gloria 2020 (Amores et al., 2020). Moreover, beach erosion will be enhanced in a climate change scenario, with rising sea levels and changes in storminess (Ranasinghe, 2016; Vousdoukas et al., 2020).

Under this threat, the implementation of effective disaster risk reduction (DRR) plans is vital for minimizing damages in settled areas (Lavell et al., 2012). A key aspect of the effectiveness of the DRR measures is community preparedness allowing, for example, timely site evacuation or effective intervention prior to the approaching storm. In this regard, early warning systems (EWSs) play an important role by combining timely and accurate hazard predictions with the associated risk levels for specific coastal receptors (Harley, Valentini, et al., 2016; Lavell et al., 2012). The successful implementation and management of EWSs are one of the most cost-effective and efficient measures for DRR and the saving of lives (Adapt Now, 2019; Ciavola et al., 2014). However, these systems do not form part of many integrated strategies for coastal risk reduction, and specifically warning systems devoted to storm-induced erosion hazards due to difficulties in testing and implementation.

Two types of modeling approaches have been implemented in operational EWSs to predict changes in beach-dune profile: descriptive conceptual models (e.g., Sallenger, 2000) and process-based models (e.g., Roelvink et al., 2009)—authors are not aware of the integration of the equilibrium profile theory-based models such as the convolution model developed by Kriebel and Dean (1993) in EWSs. For instance, the “Total Water Level and Coastal Change Forecast Viewer” managed by the US Geological Survey, predicts the timing and magnitude of water levels at the shoreline and the potential impacts on coastal dunes. The empirical wave runup parameterization given by Stockdon et al. (2006) provides inputs for the storm impact scale model proposed by Sallenger (2000), which predicts the coastal response. This efficient forecast system covers coastal regions from the entire US East Coast and certain areas of the Gulf of Mexico. A similar approach was implemented in an EWS developed in the French Aquitaine Coast to provide general information on the most exposed coastal sectors at a regional scale and impact intensity at a smaller scale (Lerma et al., 2018). While this is a rapid and simple method of determining the likely effects of storms on dune systems, if a more accurate and detailed-scale prediction of the storm impacts is required, more complex models and coastal information should be considered.

Regarding the process-based modeling approach for the development of an EWS, a few studies are found in the literature (Barnard et al., 2014; Harley, Valentini, et al., 2016; Plomaritis et al., 2018; Poelhekke et al., 2016; Seok & Suh, 2018; Valchev et al., 2014, 2016; van Dongeren et al., 2014; Vousdoukas, Ioannis, et al., 2012). In all these systems, the coastal erosion component is operated by XBeach, a depth-averaged (1DV and 2DH) morphodynamical model solving cross-shore and alongshore equations for wave propagation, flow, sediment transport, and bed-level changes (Roelvink et al., 2009). Infragravity wave motions and the related wave bore that erode the dune face during storm events are simulated as well (Roelvink et al., 2009). This process-based model is more flexible, robust, and complex than conceptual models; however, it necessitates more data for model setup, must be calibrated and validated (Simmons et al., 2017), and, even with adequate computer resources, is still time-consuming. The latter aspect might represent a major limitation for an operational system as the computational time of the real-time simulations is limited to the short period between the release of successive meteo-marine forecasts (Poelhekke et al., 2016). In order to overcome this limitation, some of the previously mentioned EWSs are based on a system trained with pre-computed process-based model results (e.g., Jäger et al., 2018; Plomaritis et al., 2018; Poelhekke et al., 2016; van Dongeren et al., 2014). The main advantages of this approach are that the computational time does not have to fit in a short forecast window, while it still preserves the capabilities and robustness of a process-based model. Then, for forecast purposes, the pre-computed EWS can be conditioned with wave-surge operational systems to predict instantaneously coastal storm impacts.

These characteristics make this approach highly suitable for a real-time prediction system (Van Dongeren et al., 2014). Nevertheless, the pre-computed procedure has some limitations. First, for operational purposes, the fundamental variables that describe a storm event must be known beforehand to condition the pre-computed EWS. While storm duration can span from a few hours to more than 1 week (Arnoux et al., 2021; Castelle et al., 2015; Ferreira et al., 2019; Mendoza et al., 2011), depending on the synoptic history of the storm, many oceanographic prediction systems that can be used to condition those EWSs only deliver forecasts for 72 hr. Hence, the prediction systems might capture the peak of the storm, but the duration of some severe storms might not be available, and this increases the uncertainty in the predicted erosion. In fact, as Kriebel and Dean (1993) demonstrated with their time-dependent beach profile model shorter storms cause less beach erosion than longer storms (assuming the same wave height peak). In line with that study, several authors (Beuzen et al., 2019; Callaghan et al., 2008;

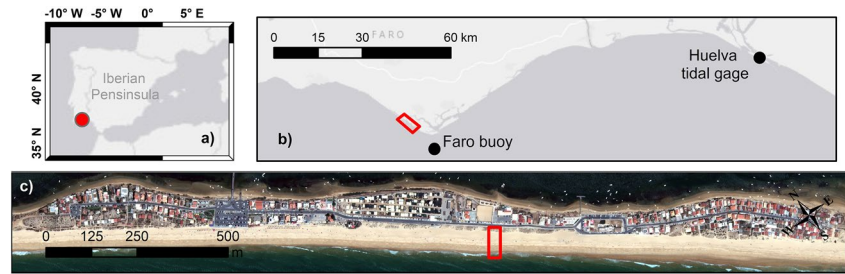


Figure 1. Location map. (a) The Iberian Peninsula with the red dot highlighting the southern coast of Portugal. (b) The location of the Ancão Peninsula (red polygon). (c) Demonstration site: Praia de Faro. The polygon highlights the location where the topographical measurements described in Section 2.2 were taken.

Poelhekke et al., 2016; Santos et al., 2019; Sanuy et al., 2018) included storm duration among the variables of their data-driven models for estimating coastal erosion. Second, the oceanic boundary information used to generate the training data set must be comprehensive enough to cover a wide range of storm conditions. Thus, as the observations do not frequently cover the full spectrum of possible storm conditions, it is a common practice to create synthetic storms (Duo et al., 2020). One of the most important aspects is the schematization of the temporal evolution of the variables that describe the storm. The most simple and widely used method is the symmetric triangular shape storm (STSS) (Duo et al., 2020; McCall et al., 2010). In this method, the unknown evolution of the variables of the synthetic events is schematized by a linear increase, until reaching the peak of the storm at half of the storm duration, with the subsequent symmetric decrease of the wave height and the corresponding surge level (Santos et al., 2019). However, this method can fail in successfully reproducing coastal erosion as seen in previous studies (Duo et al., 2020; Sánchez-Arcilla et al., 2009). Third, pre-computed simulations cannot incorporate changes in the topography/bathymetry profile (only by adding new training data). While this limitation would only apply to the pre-computed approach, in reality, most of the real-time simulations are performed by using a representative initial topo-bathymetry due to the difficulties and costs of continuously updating sea bottom information (Harley, Valentini, et al., 2016) and the subsequent integration of this information into the models. The pre-storm profile can also determine the response of a beach-dune system to coastal storms (Beuzen et al., 2019; Crapoulet et al., 2017; Mickey et al., 2020; Splinter et al., 2018), and consequently, damages in developed areas. Ferreira et al. (2019) demonstrated that a wide berm contributed to minimizing erosion-induced risks for a severe storm in a barrier island system. Moreover, differences in the modeled initial profile can be relevant when the beach is impacted by a cluster of storms and full recovery is not possible within the storm sequence. Fourthly, the inclusion of an additional variable increases exponentially the number of simulations needed to develop the pre-computed EWS.

This study hypothesized that the variability induced by storm duration and pre-storm profile is relevant for modeling erosion and retreat induced by storms. Among the uncertainties related to the schematization of the variables of a synthetic storm and their temporal evolution, the definition of the storm duration can be the most critical aspect. This aspect was tested by comparing the erosion induced by a real event with a 16-year return period against the erosion caused by synthetic events that approximated the real storm. These synthetic events had varying storm shapes, and simplifications in the duration, peak period and surge estimation. Then, the relevance of two important limitations when predicting coastal erosion induced by storms (previously unknown storm duration and representative initial beach morphology) was investigated. This research aimed to evaluate how the uncertainty related to these variables propagated into the storm-scale morphological evolution of the beach-dune system, and ultimately, contribute to building more reliable EWSs. To achieve this objective, a new methodology was developed that enabled the assessment of the importance of different variables in an EWS. The numerical experiments were designed based on hydrodynamic data and topo-bathymetry information collected in Praia de Faro, southern coast of Portugal (Figure 1a), selected as a demonstration site for this study.

2. Materials and Methods

2.1. Study Area

This numerical study was conducted at Praia de Faro, an open sandy beach located in the Ancão Peninsula (Figures 1b and 1c), at the western flank of the Ria Formosa barrier island system. The area presents a steep and

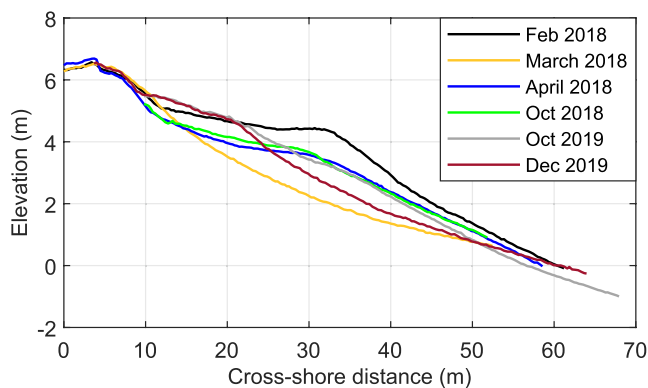


Figure 2. Example of topographical measurements referred to mean sea level, conducted in Praia de Faro between February 2018 and December 2019.

narrow beachface with a single or double berm, depending on the storm intensity and recovery conditions, that ranges in width from 15 to 40 m (Ferreira et al., 2016; Martins et al., 1996). Based on field observations, the depth of closure was established at approximately 10 m below mean sea level (MSL) (Almeida, Ferreira, & Taborda, 2011). The urbanized area is protected with buried rocks/walls or a natural beach-dune system. Sediments are medium to very coarse sand with $d_{50} \sim 0.5$ mm (Vousdoukas, Ferreira, et al., 2012). Astronomical tides are semi-diurnal, with an average range of 2.8 m during spring tides and 1.3 m for neap tides, while the storm surge levels are relatively low (<1 m) (Almeida et al., 2012). Therefore, tide conditions are more important in influencing the maximum water level than the surge itself (Fortunato et al., 2016). The wave climate has an average annual offshore significant wave height (H_s) of 0.92 m, with the 70% of the waves arriving from W to SW (71%) and the 23% from E to SE (Costa et al., 2001). Due to the cusped shape of the Ria Formosa, the site is exposed to the W–SW dominant conditions, whereas it is relatively protected from E to SE conditions.

2.2. One-Dimensional Profile Definition

Beach topography and bathymetry, oceanic conditions, and sediment sampling have been collected since the 1990s at the study site and this information was used to define the pre-storm profiles tested in this numerical study. Thus, previous authors have classified the site based on the conceptual model of Masselink and Short (1993) as reflective to intermediate (e.g., Almeida, 2007; Ferreira et al., 1997; Haerens, 2009). The beach state at Praia de Faro is highly dependent on the tidal cycle; at high tide, when the beachface is attacked by the waves, the beach is reflective, and during low tide, the beach usually exhibits an intermediate state (Ferreira et al., 1997; Haerens, 2009; Martins et al., 1996). The dominant beach morphologies are mainly low tide terrace + Rip (LTT) and longshore bar trough (LBT), as defined by Masselink and Short (1993) associated with changes in the energy conditions (Almeida, 2007; Ferreira et al., 1997; Haerens, 2009; Martins et al., 1996). The LTT profile is the predominant profile but the type of the profile depends on the combination of the pre- and post-storm wave conditions and the seasonal variation in the wave climate (Martins et al., 1996). The longshore submerged bar is built under high-energy conditions. Then, under less energetic wave conditions, sediment from the bar is landwards transported to build a berm or a terrace (Almeida, Ferreira, & Pacheco, 2011). If the wave energy is very low, the bar-trough system stays in position, limiting the recovery of the berm or terrace as observed by Almeida (2007) and Haerens (2009). Therefore, sediment lost from the beachface is gained by the sub-tidal terrace, and vice-versa, depending on wave energy (Almeida, Ferreira, & Pacheco, 2011). Both the LTT and the LBT features are situated below -1 m MSL (Haerens, 2009). The slope of the low tide terrace can range from 0.06 (Martins et al., 1997) to 0.03 (Almeida, 2007). The latter work found that the slope of the longshore bar trough is about 0.02.

The emerged profile at the site is characterized by the presence of well-developed beach cusps which induce certain variability in the beach profile (Balouin et al., 2000; Vousdoukas, 2012; Vousdoukas, Almeida, & Ferreira, 2012). The beach recovery response is very active after high-energy events, with the rapid creation of berms or the widening of the existing ones (Malvarez et al., 2021; Sá-Pires et al., 2006). The average beachface slope ($\tan \beta$) observed by various authors varies between 0.11 (Ferreira et al., 1998) and 0.14 (Ciavola et al., 1997). Moreover, differences in beachface slope between seasons are less than 0.08 (Haerens, 2009). Also, pre- and post-storm profiles tend to pivot around a point situated between $+0.5$ m MSL and -0.5 m MSL (Anfuso & Ruiz, 2004; Sá-Pires et al., 2006). Some portions of the dune line can remain stable at least for events of a 15-year return period (Ferreira et al., 2019; J. L. Garzon et al., 2022).

To model the system response sensitivity to beach morphology, different profiles that cover the natural variability observed in the field were designed. That was further supported by the information collected during a monitoring period between 2018 and 2019 that evidenced the historically observed natural beach variability of this site (Figure 2). Post-storm conditions (March 2018) were not considered to define the initial (pre-storm) profiles. Details on the monitoring program can be found in Ferreira et al. (2019), J. Garzon et al. (2020), and Malvarez et al. (2021).

Four profiles that illustrated different emerged beach morphologies were implemented in the numerical model: full high berm, eroded high berm, full low berm, and eroded low berm (Table 1; Figure 3). The submerged part of the profiles was characterized by a longshore bar and a trough as reported in the literature and also observed in the

Table 1
Sand Volume (m^3/m) Measured Between 3,680 m (MSL) and 3,740 m (Dune), Beachface Slope, Dune Characteristics (m), and Berm Characteristics (m)

	Alongshore bar and a trough (LBT)				Low tide terrace (LTT)	
	Full high berm	Eroded high berm	Full low berm	Eroded low berm	Full high berm	Full low berm
Subaerial volume	223	190	197	182	223	197
Beachface slope	0.16	0.12	0.12	0.11	0.16	0.12
Dune width	14	14	16	16	14	16
Dune toe elevation	5.0	5.0	4.5	4.5	5.0	4.5
Berm width	20	10	16	12	20	16
Berm edge elevation	4.4	4.7	3.6	3.6	4.4	3.6

2018 bathymetric survey conducted within the COSMO program (PROGRAMA COSMO, 2018). Additionally, two other profiles were evaluated, whose emerged parts represented a full high berm and full low berm profile, and the submerged part corresponded to LTT (Figure 3).

2.3. Synthetic Events at Praia de Faro

The uncertainties in the beach-dune system response were investigated by quantifying the erosion caused by synthetic storms with wave heights associated with different return periods T_R (<1, 5, 10, 25, and 50 years). The expression presented in Pires (1998) for SW events was used to compute the H_s associated with those return periods (Table 2). The rest of the variables defining the storm such as peak period (T_p), storm duration, and storm surge were estimated by using empirical formulations derived from data collected by the Faro buoy, placed at 93 m depth near Praia de Faro, and a less than 100-km distant tidal gage (Huelva, Spain) (Figure 1b), whose tidal range is similar to Praia de Faro. Previous studies have highlighted the dependence between wave height and those variables for this coastal area (Almeida et al., 2012; Poelhekke et al., 2016; Rodrigues et al., 2012). For example, Poelhekke et al. (2016) found that the relationship between max H_s and surge and duration was statistically significant with r-squared values of 0.41 and 0.54, respectively. Thus, they fitted marginal distributions of observations measured at the Faro buoy, and in combination with copulas that describe the max H_s -duration pair, generated multiple synthetic pairs of these variables. Copulas are mathematical tools that can be used to construct distributions while preserving the natural variability of the observations (Davies et al., 2017; Poelhekke et al., 2016). Following this approach, one hundred synthetic pairs of max H_s -duration were generated here. The data revealed a statistically significant relationship between these two variables (R -squared = 0.81; $p < 0.05$) as displayed in Figure 4. This correlation allowed us to obtain a linear relationship that described the storm duration as a function of the wave height. Also, to cover the possible range of storm durations for each specific wave height, the 95% confidence bands were estimated (Figure 4). Thus, for each return period and associated wave height, three storm durations were considered: low (duration 1) and high (duration 3) corresponding to the respective confidence boundaries, and the intermediate (duration 2) from the fitted expression using least squares regression (Table 2). Note that for the 1-year event only durations 2 and 3 were considered. Total water levels were computed as the combination of the astronomical tide and storm surge. For the former, typical spring tide time-series of the study site were extracted from Plomaritis et al. (2018), while for the latter, the relationship between max H_s and max surge established for this site by Rodrigues et al. (2012) was used.

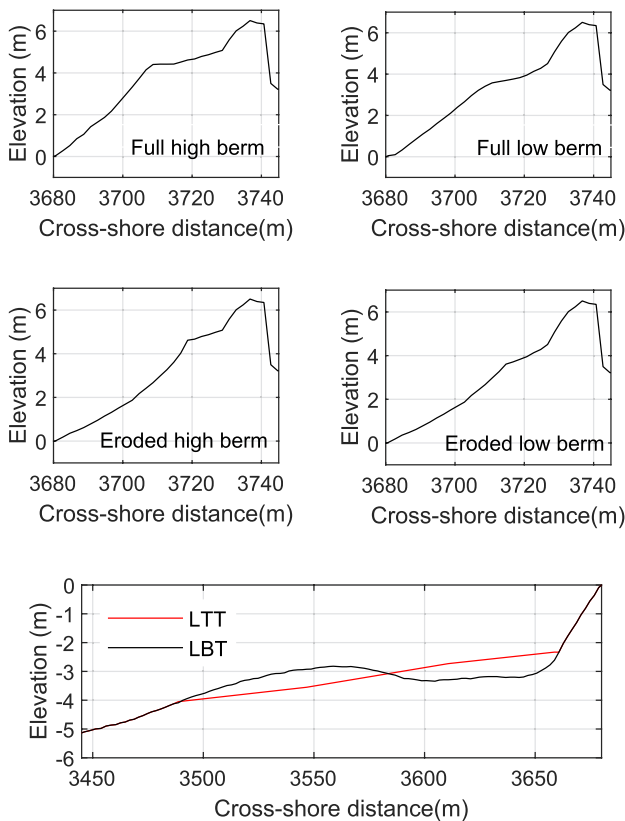


Figure 3. Morphology of the simulated profiles including emerged and submerged (LBT—alongshore bar and trough and LTT—low tide terrace) typologies. The cross-shore distances are relative to the offshore boundary of the numerical model.

Table 2
Modeled Events Characteristics

	Return period (year)				
	<1	5	10	25	50
Max Hs (m)	3	5.7	6.4	7.4	8.1
Max Tp (s)	9	11.63	12.18	12.91	13.39
Mean direction (deg)	232	232	232	232	232
Max Surge (m)	0.16	0.46	0.54	0.65	0.72
Tide ^a	Spring tide	Spring tide	Spring tide	Spring tide	Spring tide
Duration 1/2/3 (hour)	-/3/27	50/81/112	68/102/135	95/130/166	113/151/188

^aTide level #3 at Plomaritis et al. (2018). Maximum tidal range 2.42 m.

The data used to build the expression that relates H_s and T_p were collected between 1993 and 2019 and include only W-SW storm events ($H_s > 2.5$ m, according to Almeida et al., 2012) with at least 3 hr of duration. The storms that arrive from a different direction don't cause major damage to this site due to their limited fetch and site orientation. Wave height, and the associated peak period data, were clustered in 0.5 m wave height bins. Subsequently, the mode of the values of H_s and T_p within each bin was calculated. Following previous works that found an exponential relation between H_s and T_p (Mangor et al., 2017), a power expression as a function of the wave height was fitted to the mode data using least squares regression (Figure 5). The expression shown in Figure 5 was used to compute the T_p associated with the maximum H_s during the storm.

Peak periods, significant wave heights, and surges are subject to evolution over the course of an event. The unknown evolution in the synthetic events of the H_s and surge was schematized by following STSS (Duo et al., 2020). The T_p during the peak of the storm was computed by using the expression shown in Figure 5, but its temporal evolution was computed by assuming constant wave steepness (S) calculated during that peak (Plomaritis et al., 2018; Poelhekke et al., 2016). Comparisons between actual storms and their schematized events were shown in the Supporting Information (Figure S1 in Supporting Information S1), and they revealed that the simplifications used here provided a good approximation of real storms. A summary of the main variables representing each storm event is displayed in Table 2.

2.4. Uncertainty Related to the Storm Simplification Method

In order to test the initial hypothesis and quantify how the uncertainty associated with the approximation of the storm variables influenced coastal erosion, the erosion simulated for storm Emma (reference case, Run00) was

compared against erosion computed by a set of numerical tests with varying storm shape, peak period, storm surge and duration. Therefore, this comparison attempted at assessing if the symmetrical and asymmetrical triangular evolution and the computations of the peak period, surge, and duration had an impact on the final model results with respect to the reference case. To investigate if the beach morphology might affect this assessment, the topography used in the simulations of the reference case and the tests were the full high berm and the eroded low berm profiles (profiles with very distant morphologies). The main characteristics of the running tests are shown in Table 3 and Figure 6. The peak of the H_s for storm Emma was 6.55 m and it occurred at 37 hr from the beginning of the storm (considering a H_s threshold of 2.5 m). The T_p at that time was 12.5 s. The peak of the surge was 0.6 m and it occurred at 27 hr from the beginning of the storm. The total duration of the storm was 98 hr. The run01, run02 and run03 used a triangular shape to represent the H_s evolution, with the peak (6.55 m) centered in the middle, in the first quart, and the third quart of the storm duration respectively (Table 3 and Figure 6). The rest of the variables used in the simulations had the same values as the reference case. In run04, only the T_p of the storm was modified. The wave steepness was calculated based on the H_s and the T_p at the peak of

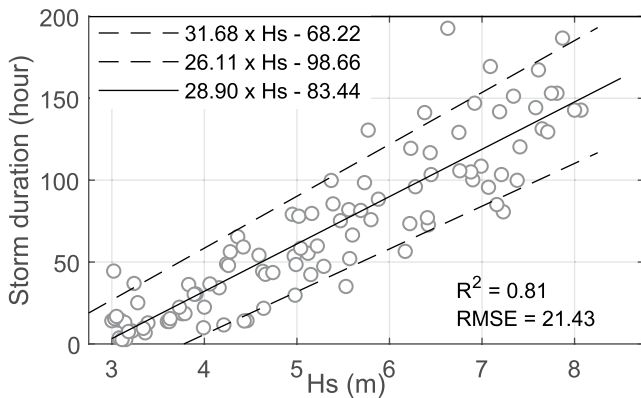


Figure 4. One hundred synthetic events created by the methodology developed in Poelhekke et al. (2016). The solid line represents the linear adjustment between wave height and storm duration and the dashed lines the 95% confidence bounds.

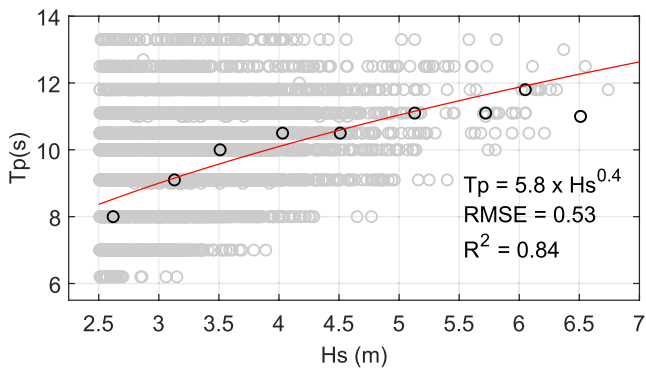


Figure 5. Relationship between H_s and T_p for W-SW storm waves (gray circles) and the statistical skills of the fit (red line) to the mode data (black circles): root-mean-square-error and R-square.

the storm (37 hr). Then, for each value of H_s and assuming that S maintained constant through the entire storm, the temporal evolution of T_p was obtained. In run05, only the surge of the storm was modified and it was obtained based on the relationship presented by Rodrigues et al. (2012). In run06, the storm duration considered (66 hr) was calculated from the equation Figure 4 (duration 2), and the time interval of the observed H_s and T_p narrowed accordingly (Figure 6). The total water levels used in the simulation corresponded to the observed values until 66 hr.

2.5. Numerical Model Framework Validation

A multi-model framework, SWAN (Booij et al., 1999) coupled with XBeach X 1.23.5526 version (surfbeat), was used to propagate the wave conditions from offshore to the shore and simulate morphological changes in the beach and dune system. A structured rectangular grid was used to perform the SWAN simulations. This grid covered the entire southern Portuguese coast to avoid the effects of the lateral boundaries. The offshore south boundary was

located at 36.905 N to lay at the location of the Faro buoy, and between 8.95 and 7.50 W where the water depth ranges between 70 and 700 m, with a mean water depth of 200 m. The sea-bottom elevation was extracted from the open data set MIRONÉ (Luis, 2007). The grid resolution was approximately 350 and 600 m in the cross-shore and alongshore directions, respectively. The model was forced at the southern boundary with the temporal evolution of the spectral bulk wave parameters. Default values were used for the model parameters that govern the wave propagation. Water level variations and wind effects were not considered in the simulations. Model outputs were extracted at 25 m depth to pass the information to the XBeach model. The 1D XBeach grid had a variable cross-shore resolution with a minimum node spacing of 2 m in the surf zone and emerged profile. Because wave measurements in the surf and swash zone were not available, wave breaker parameters were inspired by values found in the literature (Do et al., 2018; Plomaritis et al., 2018) as displayed in Table 4. Also, Garzon et al. (2022a) found that the scheme selected to simulate the propagation of the directionally spread short wave groups in XBeach can impact the dune erosion. Here the option considering wave refraction (multi_dir) was implemented. The model was calibrated by using variations in three model parameters: facua (parameterized wave asymmetry and skewness sediment transport component), bermslope (upslope transport term for semi-reflective beaches), and wetslope (critical avalanching submerged slope) because they have been found to largely impact the erosion of the steep profiles similar to those assessed here (Cho et al., 2019; J. L. Garzon et al., 2022a, 2022b; Simmons et al., 2019; Vousdoukas, Ioannis, et al., 2012).

Topographical measurements collected after the impact of the storm Emma (Ferreira et al., 2019), were used to assess the performance of this numerical framework. The comparison between the modeled and measured post-storm profiles were shown in Figure 7 along with the statistical skills. The evaluation metrics namely, Brier Skill Score (BSS), root-mean-square-error (RMSE), and bias indicated an excellent model performance regardless of the submerged profile considered in the modeling. Therefore, this model setup satisfactorily reproduced

Table 3
Modeled Events Characteristics to Assess the Storm Simplification Method

Run	Tide	Surge	Duration	H_s	Storm shape	T_p
Run00	Observed	Observed	Observed	Observed	Observed	Observed
Run01	Observed	Observed	Observed	Observed Peak	STSS	Observed
Run02	Observed	Observed	Observed	Observed Peak	Asymmetrical triangular shape—1/4 of the duration	Observed
Run03	Observed	Observed	Observed	Observed Peak	Asymmetrical triangular shape—3/4 of the duration	Observed
Run04	Observed	Observed	Observed	Observed	Observed	Constant S based on the max H_s and the simultaneous T_p
Run05	Observed	Rodrigues et al. (2012)	Observed	Observed	Observed	Observed
Run06	Observed	Observed	66 hr	Observed	Observed	Observed

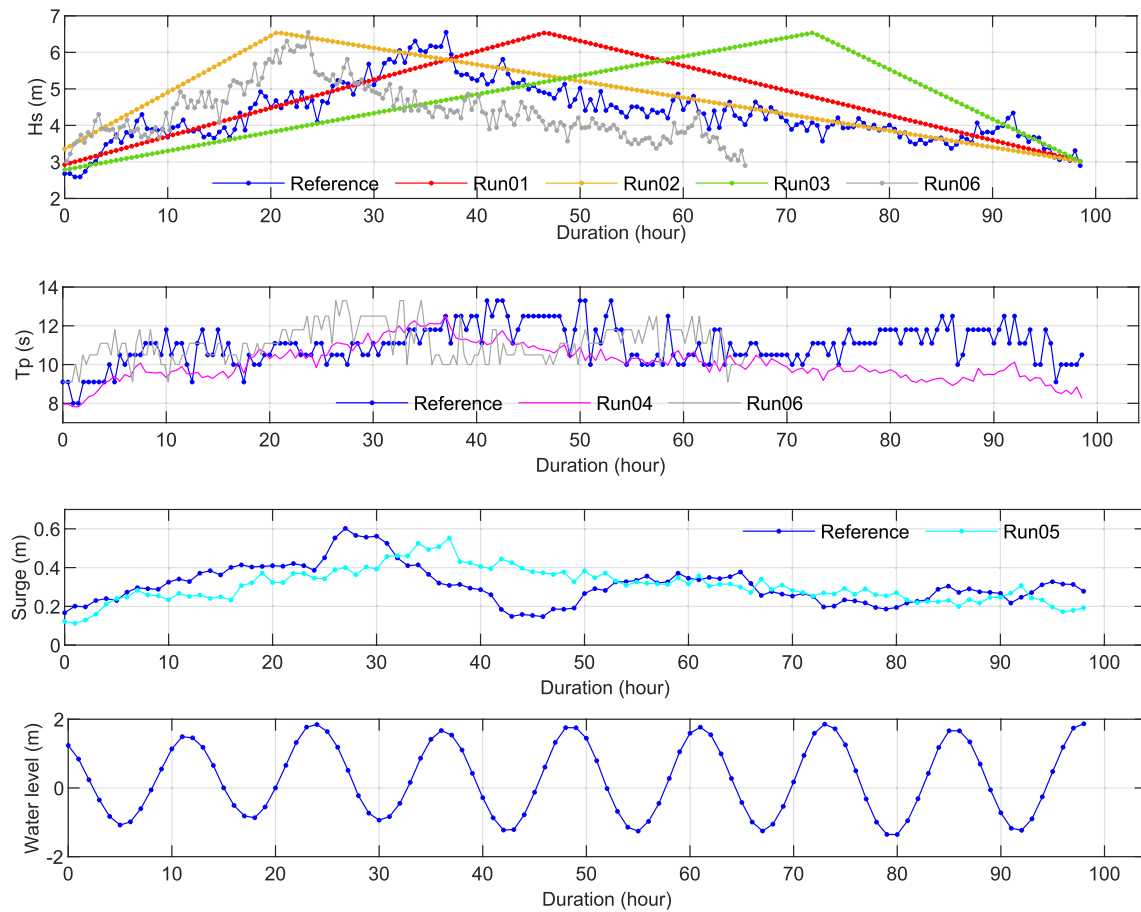


Figure 6. Oceanic conditions used to assess the accuracy of the storm simplification method.

morphological changes when the model was initialized with any of these two submerged morphologies. The calibrated model was validated for other locations along the Praia de Faro, some of them revealing dune erosion, yielding BSS values ranging from 0.86 to 0.96. A detailed explanation of the model validation is provided in Figures S2 and S3 in Supporting Information S1.

2.6. Erosion Indicators

Three erosion indicators that are relevant for coastal erosion warning systems, in line with those presented by Ferreira et al. (2017), were included in the analysis: (a) eroded volume of the subaerial region, in absolute and relative terms, computed from MSL (3,680 m from the offshore boundary of the XBeach model) to the back-side of the dune system (3,740 m); (b) the absolute and proportional berm retreat. The latter was estimated as the distance between the initial and final berm edge (berm retreat) compared to the initial berm width and; (c) absolute and proportional dune retreat. The latter was estimated as the horizontal profile retreat at the elevation of the pre-storm dune toe (dune retreat), compared with the initial dune width. In addition, the suitability of the storm impact regime developed by Sallenger (2000) to predict berm and dune impacts was analyzed by using the simulated maximum water levels and the post-storm dune/beach morphology. It intended to understand the effectiveness of the storm impact regime method (morphological static thresholds) to characterize the impacts against the modeling approach, which considers morphologic time-varying thresholds.

3. Results

3.1. Uncertainty Related to the Storm Simplification Method

The tests used to investigate the suitability of the triangular shape simplification (Run01-Run03) revealed that the maximum differences in the eroded volume reached approximately 10% and 5% for the eroded low berm

Table 4
Main Numerical Parameters and Their Values

Parameter	Value
Breaking formula	roelvink2
Gamma	0.545
Gamax	2.36
Delta	0.1
Beta	0.138
Alpha	1.1
Facua	0.15
Wetslope	0.45
Bermslope	0.12
Turb	wave_averaged
Single_dir	Off
Lateral flow condition	Neumann
Morfac	10
Factor bed slope effect	0.15
dz_{max}	0.05
h_{switch}	0.01
Manning's coefficient	0.02
Dryslope	1

profile and full high berm profile, respectively, in Run03 when compared to Run00 (Figure 8a). For the rest of the shape simplifications evaluated, the eroded volume of Run02 (asymmetrical triangular shape—1/4 of the duration) only differed from the reference case by 3.5%, while the eroded volume of the STSS only deviated from the reference case by 4%. The analysis of the proportional berm and dune retreat showed that, in the reference case and the numerical tests, the berm was fully eroded in the simulation initialized with the eroded low berm profile and that the dune was not impacted in the simulation initialized with the full high berm profile (Figure 8b). In the tests Run01–Run03, differences in the proportional berm retreat with respect to the reference case varied between -14% and $+14\%$, while differences in the proportional dune retreat ranged between 13% and 26% (i.e., all the tests computed more dune retreat than the reference case). In Run04, used to evaluate the effectiveness of the definition of the T_p , the maximum difference in eroded volume and proportional dune retreat with the reference case were 14% and -17% , respectively (Figure 8). In both runs, the test and the reference case computed the same proportional berm retreat. The test that evaluated the approximation used to calculate the storm surge (Run05) computed 5% more eroded volume than the reference case (Figure 8a). The proportional berm and dune retreat were also higher, 14% and 8%, respectively (Figure 8b). The expression used to compute the storm duration based on the maximum $\langle H_{si} \rangle$ provided a duration of 66 hr, 32 hr shorter than the actual duration of the storm Emma. Thus, Run06 simulated between 27% and 32% less eroded volume (depending on the beach profile), 28% less proportional berm retreat, and 65% less proportional dune retreat than the reference case (Figure 8). These results demonstrated that, with the exception of Run06 (smaller duration), all other tests provided reasonable (up to 25%

difference) to very good (less than 5% difference) variations with respect to the reference. Therefore, the following sections focused on assessing how the uncertainties related to storm duration and initial beach morphology impacted coastal erosion using synthetic storms.

3.2. Variability and Uncertainties Due To Beach Morphology

The variability in the indicators due to the pre-storm beach morphologies (Figure 3) was evaluated by analyzing the post-storm profiles simulated using events with duration 2 (linear adjustment, see Table 2). For the 5-year event, when model runs were initialized with the high berm morphologies (full and eroded), final profiles exhibited a 2-m scarp that clearly defined the edge of the remaining berm (Figure 9). Also, the post-storm berm remained wider for the case of the full high berm, as displayed in Figure 9. Conversely, the berm was fully depleted after this event on the profiles that exhibited lower berm height, regardless of the berm width (Figure 9). For the 10-year event, only the full high berm profile maintained a short berm after the storm (Figure 9). In the eroded high berm profile, the berm was fully depleted after the event, but the erosion did not reach the dune. On the contrary, limited dune retreat was observed in the low berm profiles, as displayed in Figure 9.

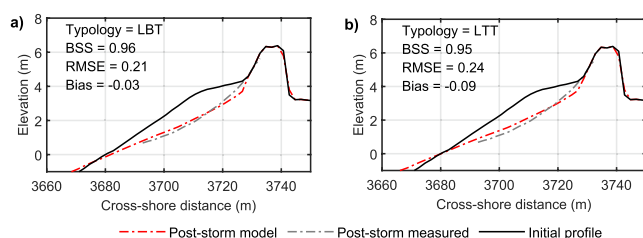


Figure 7. Initial, measured, and simulated profiles used for model calibration and statistical skills. The submerged profile is represented with (a) the longshore bar trough morphology and (b) the low tide terrace morphology.

For the 25-year event, the berm was completely depleted after the storm for all beach morphologies. Also, the post-storm dune position was very similar for all profiles (see Figure S4 in Supporting Information S1). The modeled dune retreat was approximately 4 m in the full high berm profiles, while in the rest of the profiles, the dune retreat reached 7 m (Figure 9 and Table S1 in Supporting Information S1). For the 50-year event, the dune was severely eroded (between 7 and 12 m) but it was not completely eroded for any of the morphologies (Figure 9 and Table S1 in Supporting Information S1). When the model was initialized with the profiles with the highest volume (full high berm), the retreat was the least. Moreover, no differences were found between the post-storm full low berm and eroded high berm profiles for this event (Figure 9 and Figure S4 in Supporting Information S1). For all the assessed

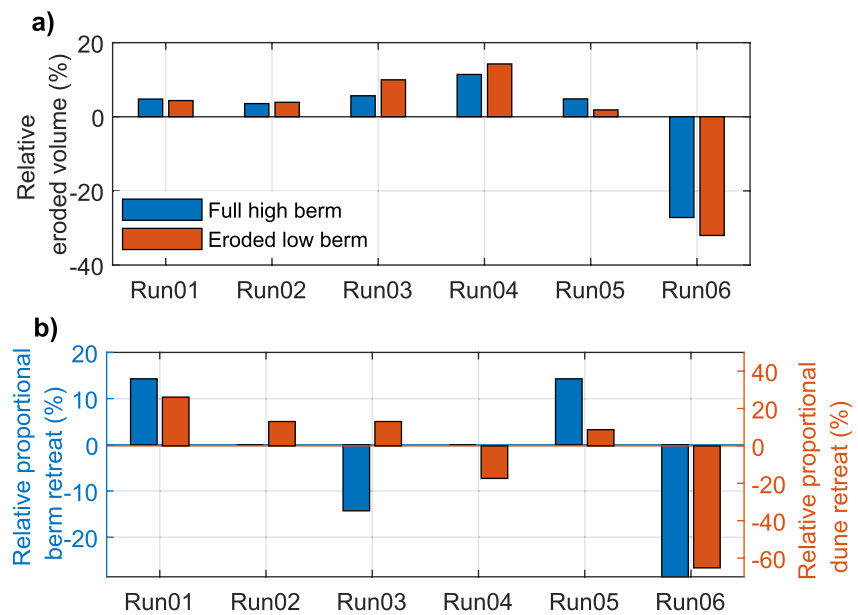


Figure 8. (a) Relative eroded volume with respect to the reference case. (b) Relative proportional berm and dune retreat with respect to the reference case. Positive values indicate that the erosion simulated is higher in the running tests than in the reference case.

events, the effect of the submerged morphology in the eroded volume, and berm and dune retreat was not relevant and it can be observed that the LTT and LBT profiles resulted in a similar post-storm profile (Table S1 and Figure S4 in Supporting Information S1).

For the 5- and 10-year events (duration 2), the morphology of the high berm profiles induced a reduction of the maximum elevation reached by the sea surface, and the storm impact regime was swash (the dune was not impacted, as displayed in Figure 9). Conversely, the flow propagated further landwards in the low berm profiles and the maximum water elevation exceeded the dune toe height (collision regime) during these events. This caused a full depletion of the berm (Figure 9). Thus, different storm impact regimes (swash and collision) were observed depending on the berm elevation for these events. However, the collision regime did not necessarily always induce dune retreat as shown in Figure 9 (e.g., 5-year event for full and eroded low berm profiles). For the 25-year and 50-year events, the maximum water levels vastly exceeded the dune toe elevation (collision regime) in all beach morphologies and it caused dune retreat for all considered profiles (Figure 9). A similar regime (collision) was modeled for all profiles under these events, but this did not differentiate the severity of the dune retreat. Regarding the maximum water level variation related to the submerged morphology, it was observed that it did not affect the maximum water elevation and therefore, the storm impact regime (Table S1 in Supporting Information S1).

The previous analysis demonstrated (in absolute terms) how each morphology individually behaved during the storms. Additionally, to investigate the overall uncertainty associated with the selection of the beach morphology, changes in relative terms, that is, with respect to each initial morphology, were analyzed. Also, the mean and the standard deviation of the erosion indicators, namely relative eroded volume, proportional berm retreat and proportional dune retreat, were calculated considering all profiles (Figure 3). The uncertainty band associated with the beach morphology (centered in the mean \pm 1.96 standard deviations) for each storm was computed (see Figure 10). Assuming normal distributions, it was expected that at least 95% of the individual runs lie within this band. For duration 2, it can be seen that the uncertainty in the relative eroded volume associated with the beach morphology is 5%–8%, regardless of the storm intensity (the width of the uncertainty band did not change remarkably with the return period). When the proportional berm retreat was analyzed, it was found that the uncertainty depended on the storm severity and it decreased with higher severity. For the 5-year event, it accounted for 85%. It indicated that for these storm conditions, the proportional berm retreat can vary from 15% to 100% (full berm depletion). For the 10-year event, the uncertainty was 22%, from 78% to 100% (full berm depletion), as indicated in Figure 10. Regarding the proportional dune retreat, the uncertainty moderately increased with storm

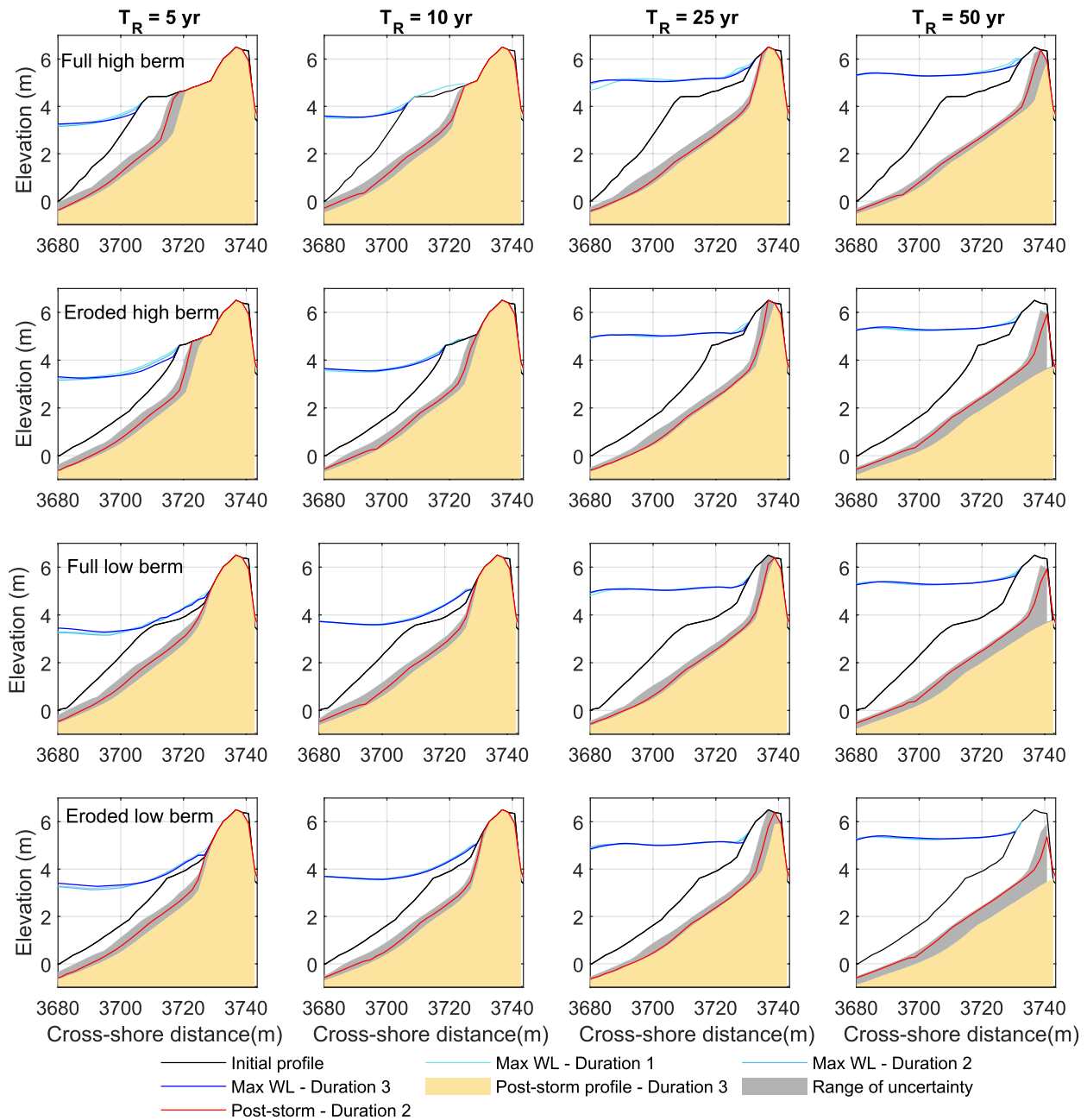


Figure 9. Simulated maximum water level (WL) and post-storm profiles for different return periods, durations, and initial morphologies (only longshore bar trough bathymetry). The blue lines (WL) are superposed to each other in most cases.

severity. Thus, it was 14% for the 10-year event (from null relative dune retreat to 14%), 30% for the 25-year event (from 23% to 53%) and 41% for the 50-year event (from 40% to 81%).

Variations in the pre-storm morphology led to changes in the absolute eroded sediment above MSL (Table S1 in Supporting Information S1). However, the relative (percentage) eroded material was similar for most profiles/conditions, regardless of the initial morphological conditions. For instance, for the 10-year event and duration 2, the sediment eroded was 61.9, 56.0, 52.1, and 51.7 m^3/m for the full high berm, full low berm, eroded high berm, and eroded low berm profiles (LBT), respectively, and 57.1 to 50.9 m^3/m for the full high berm and full low berm profiles (LTT) (Table S1 in Supporting Information S1). This corresponded to 26%–28% of the pre-storm volume for all the beach morphologies (Figure 10a). In the case of the 25-year event and duration 2, all beach profiles

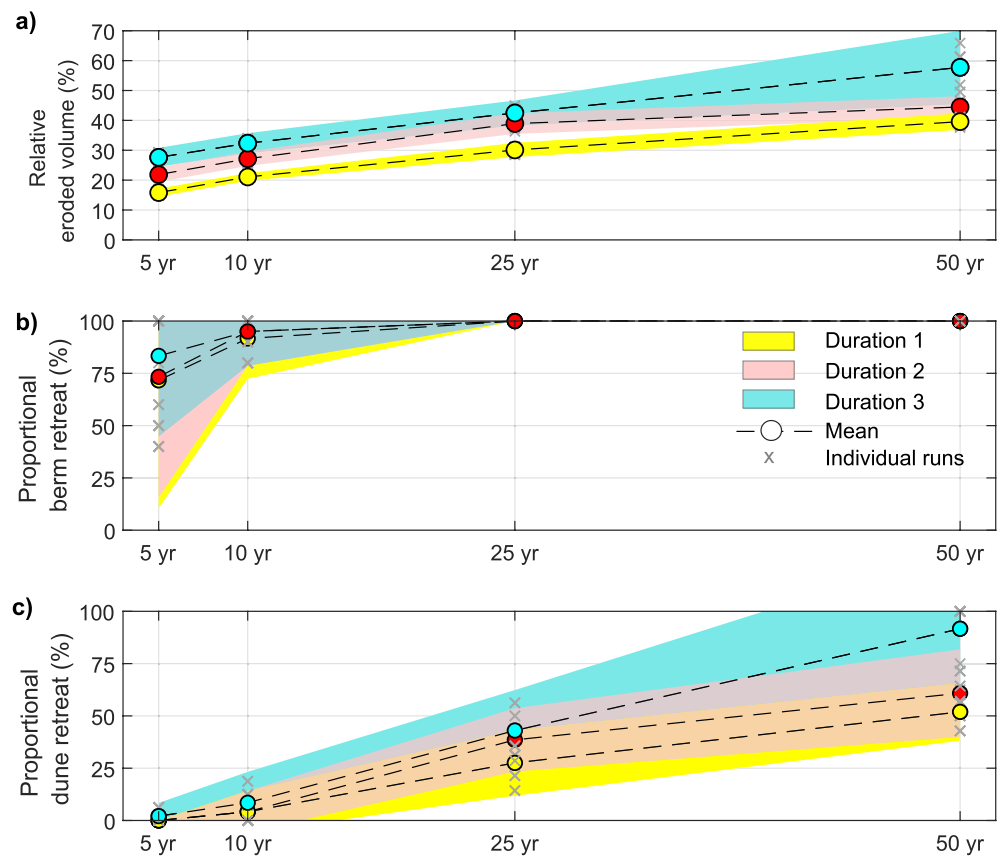


Figure 10. (a) Relative eroded volume (%). (b) Proportional berm retreat (%). (c) Proportional dune retreat (%). Each colored area represented the uncertainty band associated with the beach morphology for a given storm duration. It was centered on the mean value (each color circle) and it was extended by ± 1.96 standard deviations.

lost 36%–40% of the beach volume above MSL. This fact was depicted by the narrow bands in Figure 10a that indicated a small standard deviation of the relative eroded volume computed among the individual runs.

3.3. Variability and Uncertainties Due To Storm Duration

The storm with the lowest return period did not erode the berm for any of the two longer durations assessed and for any of the simulated beach morphologies; however, higher sand volume was eroded with the storm lasting for 27 hr (duration 3) as shown in Table S1 in Supporting Information S1. For the 5-year event, differences in berm retreat obtained for duration 1 and duration 3 simulations were only relevant in the high berm profiles, reaching up to 4 m (Figure 9 and Table S1 in Supporting Information S1) or 40% of the proportional berm retreat (between 40% and 80%) as shown in Figure 11. In the low berm profiles, all storm durations assessed resulted in berm depletion (Figure 9). The differences in the eroded sand volume between duration 3 and duration 1 were about 21–25 m³/m in all the profiles LBT (Table S1 in Supporting Information S1). This duration variability accounted for changes in the relative eroded volume of 12%–14%, as displayed in Figure 11. For the 10-year event, the berm and dune retreat were barely sensitive to storm duration since simulations with duration 1 and duration 3 led to similar results (Figure 9 and Table S1 in Supporting Information S1). Eroded volume differences were around 21–25 m³/m (11%–13% of the relative eroded volume, Figure 11). For the 25-year event, the berm was depleted in all the morphologies for the three assessed durations. Regarding the dune retreat, changes driven by duration variability were 2 m, that is, changes of 12%–15% of the proportional dune retreat (Figure 11), except for the eroded low berm profile (4 m and 25% of variations in the proportional dune retreat, Figures 9 and 11, and Table S1 in Supporting Information S1). Similar to the other events, the eroded sand volume was sensitive to storm duration and the variability of this variable induced changes in the eroded volume of 24–25 m³/m, equivalent to 11%–14% of the relative eroded volume (Figure 11). For the 50-year event, the dune retreat was very sensitive to storm duration. In the eroded high berm, full low berm, and eroded low berm profiles, only the storm with the longest duration (188 hr) caused dune removal while the events with duration

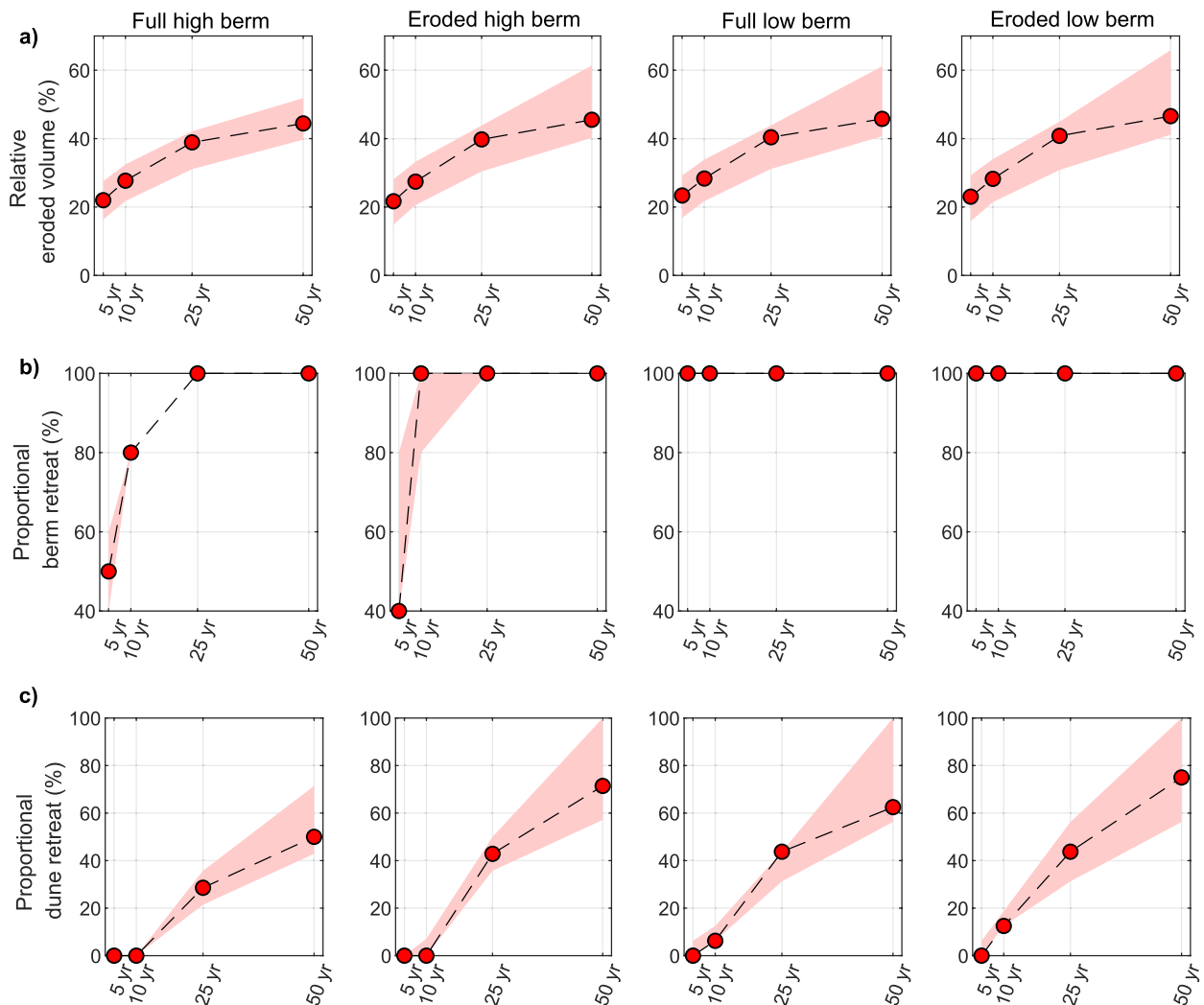


Figure 11. (a) Relative eroded volume (%). (b) Proportional berm retreat (%). (c) Proportional dune retreat (%). Each red area was centered on the indicator obtained for duration 2 (red circles) and the shadow area represents the envelope of the indicators for duration 3 and duration 1.

1 and 2 did not. In these profiles, the dune retreat variability was 6–7 m (Figure 9 and Table S1 in Supporting Information S1), that is, the duration variability led to differences in the proportional dune retreat of 44% (Figure 11). The changes in the relative eroded volume were more significant than for less energetic events (21%–24%), as shown in Figure 11. The dune retreat variability due to storm duration at the full high berm profiles was 4 m, and this accounted for 29% of the relative dune retreat differences (Figures 9, Figure 11 and Table S1 in Supporting Information S1).

The morphology of the submerged profile did not influence remarkably the sensitivity of the coastal storm indicators to storm duration, and LBT and LTT profiles exhibited a similar sensitivity range (Table S1 in Supporting Information S1). Also, the storm impact regime was not very sensitive to storm duration. However, for the 50-year event, while the maximum water levels did not exceed the initial dune crest for any of the durations, the longest storm was capable of lowering the dune crest leading to a shift in the storm impact regime (from collision to overwash). Similarly, the initial dune toe elevation was not exceeded by the maximum water levels for the 10-year event on the eroded high berm morphology, but the total erosion of the berm found for the events with duration 2 and 3 caused the lowering of the dune toe leading to a shift from swash to collision regime.

Similar to the analysis of the pre-storm beach profile, besides investigating the changes in absolute terms, the uncertainty in relative terms was also assessed. The uncertainty of the relative eroded volume to storm duration (considering the differences between the mean values of the indicators for duration 1 and duration 3) was 12% (between 15% and 27%) for the 5-year event, 11% (between 21% and 32%) for the 10-year event, 12% (between

30% and 42%) for the 25-year event, and 18% (between 39% and 57%) for the 50-year event (Figure 10a). The uncertainty of the proportional berm retreat related to storm duration was 12% (between 71% and 83%) for the 5-year event and 4% (between 91% and 95%) for the 10-year event (Figure 10b). The berm was fully depleted for all the durations for more energetic events, therefore the uncertainty is 0%. The uncertainty of the proportional dune retreat to storm duration increased with storm severity. The uncertainty was 2% (between 0% and 2%) for the 5-year event, 4% (between 4% and 8%) for the 10-year event, 16% (between 27% and 43%) for the 25-year event, and 40% (between 51% and 91%) for the 50-year event (Figure 10c).

Importantly, the results revealed that the uncertainty of the relative eroded volume associated with storm duration was higher than the uncertainty associated with the initial beach morphology (Figure 10a). However, this was not the case for the proportional berm retreat, where the variability induced by the profile was remarkably higher (Figure 10b). For the proportional dune retreat, the uncertainties related to beach profile were higher than the uncertainties related to storm duration in the 10-year and 25-year events. For the 50-year event, the uncertainties related to storm duration and beach profile obtained similar values (Figure 10c).

The pre-storm beach morphology played an important role in the morphological changes induced by storm variability. Therefore, besides analyzing changes in the mean values, variations between the uncertainty bands of the events with duration 1 and duration 3 were investigated to understand the combined uncertainty of both variables. For the relative eroded volume, the combined uncertainty was 16% (between 14% and 30%) for the 5-year event, 15% (between 20% and 35%) for the 10-year event, 20% (between 27% and 47%) for the 25-year event, and 34% (between 36% and 70%) for the 50-year event (Figure 10a). The combined uncertainty of the proportional berm retreat was 90% (between 10% and 100%) for the 5-year event and 28% (between 72% and 100%) for the 10-year event (Figure 10b). The combined uncertainty for the proportional dune retreat was 8% (between 0% and 8%) for the 5-year event, 9% (between 14% and 23%) for the 10-year event, 50% for the 25-year event (between 12% and 62%), and 62% (between 38% and 100%) for the 50-year event (Figure 10c).

4. Discussion

4.1. Model Performance

The impact of storms in Praia de Faro has been previously investigated by numerical experiments and field observations. Almeida, Ferreira, and Taborda (2011) implemented the convolution model (Kriebel & Dean, 1993) along 26 cross-shore profiles to evaluate the vulnerability of this site under the impact of the 25-year event and they obtained minimum, maximum and average dune retreats of 2.5, 15, and 8 m, respectively. The dune retreats found in the present experiment were generally lower for the same return period, ranging between 3 and 9 m. Ferreira et al. (2006) also applied Kriebel and Dean's approach to compute the retreat driven by the 50-year event yielding values of 25 m approximately. This would mean the full removal of the dune and erode a part of the urbanized area. The retreat found in their study exceeded the one computed here (Table S1 in Supporting Information S1), where dune depletion was only found for the longest storm (188 hr). Larger retreat provided by the convolution model with respect to the XBeach model was also observed by Plomaritis et al. (2019). The discrepancies between both models can be the consequence of the different approaches to compute coastal erosion: analytical against process-based. While top-down models such as the convolution model are computationally efficient (Ferreira et al., 2018; Plomaritis et al., 2019) and thus with a great utility for first assessments, process-based models are more accurate and robust (Callaghan et al., 2013) and should be used for detailed risk assessments, including a local EWS, whether computationally power is not a major limitation.

Regarding field observation studies, the impact of the storm Emma, a 16-year return event considering just Hs and more than 20 years if the joint probability between waves and surges is considered (Ferreira et al., 2019), caused dune retreats up to 3 m along the Praia de Faro (J. L. Garzon et al., 2022). Considering that the profile before the arrival of the storm can be classified as a full high berm profile, the observations and the currently used model results agreed well (Table S1 in Supporting Information S1). Also, this study corroborated that the STSS approach was valid for this study site (only for SW storm directions).

4.2. Variability and Uncertainties Due To Beach Morphology

The response of the beach to the 5-year event was conditioned by the berm volume and height. After the formation of the initial beach scarp, the incoming wave energy caused the undercutting of the scarp leading to a migration upwards and landwards of the scarp toe in all beach morphologies. Then, in the low berm profiles, the lower

elevation enabled the maximum water levels to easily exceed the scarp crest (Figure 9) during the course of the storm removing this near-vertical feature, similar to the process described by van Bemmelen et al. (2020). Importantly, this occurred before the peak of the storm was reached and the new-formed gentler slope facilitated the inland propagation of the flow, extending the maximum water levels close to the dune toe. As the flow propagated landwards, the berm was more intensively eroded. On the other hand, in the high berm profiles, the maximum water levels did not exceed the scarp crest during the storm (Figure 9). Thus, the scarp obstructed the uprush, and the flow did not propagate further inland, limiting the erosion to the seaward side of the scarp (see Supporting Information for an illustration of the profile and water level evolution). These two different scarp evolutions were also observed by van Bemmelen et al. (2020) who also declared that beach scarps are prone to be formed in high platform elevations and steep initial beach slopes. Also, according to previous formulations that relate beach slope and runup (e.g., Stockdon et al., 2006), for beaches with uniform slope, one might expect that the full high berm profile simulation revealed the highest total water levels as it had the steepest beachface slope. However, the formation and maintenance of the scarp determined the maximum water elevation that did not reach the dune toe as occurred with low berm profiles. Therefore, the pre-storm beach morphology determined the berm erosion and the overall regime. This was also highlighted by Mickey et al. (2020) who stated that pre-storm barrier island morphology (with identical dune toe and crest elevation) can cause differences in storm regimes.

For the 10-year event, a well-marked berm scarp was initially created but the maximum water levels rapidly exceeded the scarp crest leading to its removal in the low berm profiles (Figure 9). As the storm continued, the berm was progressively eroded, and the low berm profiles represented an insufficient sand buffer to protect the dune which promoted its retreat (see Supporting Information). Conversely, the larger berm elevation of the high berm profiles avoided the total berm depletion, protecting the dune from erosion (Figure 9). As found in previous studies, here the berm robustness inversely determined the dune erosion (Beuzen et al., 2019; Crapoulet et al., 2017; Fairley et al., 2020; J. L. Garzon et al., 2022). Moreover, the newly formed gentler slope of the low berm profiles also contributed to farther extend inland the maximum water level, and along with the lower dune toe elevation, allowed the total water levels to exceed the dune toe (collision regime). When waves exceeded the dune toe, the incoming swash wave energy collided with the dune resulting in dune erosion. Beuzen et al. (2019) stated that dune erosion is equally affected by the exceedance of the total water levels above the dune toe and the width of the berm immediately fronting the dune (wider beaches result in a reduction of dune erosion).

For the 25- and 50-year events and all morphologies, the total water levels rapidly reached the dune toe elevation and waves collided with the dune (Figure 9). During these highly energetic events, the dune retreat was mainly controlled by the available sand volume as the full high berm profile (150 m³/m) reduced the dune retreat with respect to the rest of the profiles. For the eroded high berm and full low berm profiles, whose sediment volume was similar (117 and 115 m³/m), the final post-storm position was very similar after those very energetic events. Also, the eroded low berm profile, with the lowest sediment volume (100 m³/m), was the most eroded one. This demonstrated the importance of the pre-storm sand volume (beachface and backshore) in affecting the response of the beach-dune system, in line with other works (J. L. Garzon et al., 2022; Guisado-Pintado & Jackson, 2018). If the profiles maintain approximately the same sand volume, even for different morphologies, the post-storm profile is very similar, especially for very high energetic events, as stated by J. L. Garzon et al. (2022a). On the other hand, the LBT and LTT morphology did not alter the erosion indicators notably for any of the events, and minimal changes were only observed in sand eroded volume, with larger eroded volume found in the LBT profiles in relation to the LTT profiles. This is in line with Splinter and Palmsten (2012) who investigated the effect of a range of bathymetries in modeling sub-aerial beach erosion and concluded that XBeach was not very sensitive to variations in the offshore bathymetry.

It is important to underline that conversely to observations on sandy beaches, and specifically, in the study area (Almeida, Ferreira, & Pacheco, 2011), that have revealed sandbar development in the surf zone during storms, the model did not simulate the formation or the growth of these submerged features but the accumulation of sediment in the submerged region until 3 m below MSL (Figure S5 in Supporting Information S1). This possible lack of skills in modeling morphological changes below MSL has been previously reported (Kalligeris et al., 2020; Vousdoukas, Ioannis, et al., 2012). It is worth mentioning that reproducing sandbar development and offshore migration during the storm was not intended in the present study as the modeling of these processes would demand a specific calibration as noted by previous studies (Kalligeris et al., 2020; Rafati et al., 2021; Suzuki & Cox, 2021). However, even if the model failed in simulating the evolution of the submerged profile, the model results can be still reliable in the beachface region, as displayed in Figure 7.

In terms of berm volume eroded, profiles whose berm had more material, lost more sediment. This was also reported by Harley, Turner, et al. (2016), Scott et al. (2016), and Beuzen et al. (2019) who stated that the pre-storm profile was fundamental to determining the berm erosion, with more accreted berms facing larger erosion. However, the percentage of the eroded volume of the subaerial region was not affected by the pre-storm morphology, and for each specific storm, the relative eroded volume was very similar across the profiles (Figure 10). This agreed partially with Harley, Turner, et al. (2016) observations of berm erosion along a 3,500 m coastal stretch after two virtually identical storms. The authors declared that the beach response, in terms of berm erosion, as the percentage of the pre-storm berm volume, was very similar in these two events. In this study, the percentage of the berm eroded volume (measured from the MSL to the dune toe) varied across the profiles (not shown); however, the percentage of the eroded volume computed in the entire subaerial region (above MSL) of the beach at those profiles was very similar. Moreover, the percentage of eroded volume and return period can be fitted by a power-law expression, as illustrated in Figure 10a, similarly to suggested by other authors (e.g., Eichtenopf et al., 2019; Ferreira, 2005). Likewise, Splinter et al. (2014) used a power-law relationship to represent wave energy density and eroded dry beach volume.

4.3. Variability and Uncertainties Due To Storm Duration

The effect of the storm duration on the berm and dune retreat indicators was different based on the storm severity and beach morphology. In the 5-year event, the storm duration had an impact on the berm retreat of the high berm profiles, but not on the other beach morphologies (on these profiles the berm was completely eroded regardless of the duration), as shown in Figure 9. On the other hand, the berm and dune retreat were barely sensitive to storm duration in the 10-year event for any of the morphologies. In the 25- and 50-year events, the dune retreat response to variability in storm duration was more sensitive. This is especially remarkable for the 50-year event, where the storm duration regulated the capacity of the dune to endure. Thus, with the longest storm, some of the profiles reached a tipping point in which the dune was completely eroded and a possible positive feedback mechanism can be initiated leading to breaching and the possible occurrence of the inundation regime.

The importance of the storm duration on coastal erosion is widely accepted. For instance, based on field observations, Cohn et al. (2019) found an increase in dune eroded volume with increasing storm durations. Similarly, Beuzen et al. (2019) declared that if the dune toe were exposed to wave action during longer periods, the dune eroded volume and dune retreat also increased. Using numerical models, Sánchez-Arcilla et al. (2009) calculated the eroded volume variability by estimating the difference between computations for a given wave height with varying duration. As in the present experiment, a linear relationship was fit between H_s and duration. They found that the influence of the storm duration on the erosion increased with larger wave heights because the range of durations was wider for more energetic waves, from 15 hr (the less energetic event) to 40 hr (the most energetic event). The results presented here displayed another pattern, and the differences in eroded volume resulting from the 5-, 10- and 25-year events with varying storm duration were almost constant. A similar range of durations for all events, ± 30 hr (Table 2), can be the reason for this model's response to storm duration. However, other indicators such as dune retreat became more sensitive to storm duration with increasing storm severity (25- and 50-year events).

For some of the events, the storm impact regime varied with the storm duration, as longer storms were able to lower the dune toe or the dune crest leading to a shift in the storm impact regime. Therefore, accounting for the time-varying morphologic changes during the course of the storm, such as downwards migration of the dune toe and dune avalanching, can be critical to correctly predicting the storm impact regimes. This corroborated the findings presented by Mickey et al. (2020) in their numerical experiment on a barrier island.

In the numerical study conducted by Plomaritis et al. (2018) in Praia de Faro (using a full berm profile morphology) the authors concluded that the storm duration did not provide additional information to their probabilistic model and that this variable did not succeed in predicting hazard or no-hazard storm situations. They argued that the copula method used in the study to relate wave height and duration correctly reproduced this association. Also, they found that this approach contributed to limit the number of simulations to train their Bayesian network. In the present study, storm duration did not determine the occurrence of dune retreat, but it had an impact on the dune retreat variability, especially for the most energetic event.

4.4. Implications for an EWS

Most of the EWSs (based on real-time and pre-computed simulations) consider representative morphological pre-storm conditions. On one hand, if the EWS predicts the relative eroded volume of the emerged profile,

according to the presented results and previous studies (e.g., Harley, Turner, et al., 2016), the uncertainties related to the selection of the initial beach profile are not very relevant. On the other hand, the results suggest that the uncertainty associated with the pre-storm morphology is relevant for correctly identifying tipping point conditions such as berm depletion or dune removal. For moderate events (5- and 10-year events), the pre-storm beach profile seems to be highly relevant to totally (or not) erode the berm. This indicates that if the EWS focuses on coastal receptors such as recreational activities and beach user facilities located at the backshore (as found in many sites, e.g., Armaroli et al., 2013), the risk uncertainties related to the selection of the pre-storm conditions are very high, up to 85%. This would imply possible large underestimations or overestimations of the risks depending on the actual pre-storm beach morphology. This is of particular relevance in this study area where beach cusps can induce a reasonable alongshore variability of the beach profile (partially corresponding to the high/low berm morphologies used in this study). On the other hand, if the receptors are located in the dune, the uncertainties caused by the initial beach morphology are still important but lower (up to 41%). However, the impact of the initial morphological conditions is also remarkable on dune retreat driven by extreme events (i.e., 50-year return period) since the variability associated with this parameter can lead to dune breaching and the starting of overwash to the inner areas. Taking this into account, morphology variability can be highly relevant to define levels of protection and risk reduction actions.

Many storm impact prediction systems rely on static morphological indicators. Nevertheless, the time-varying morphological changes during a storm can determine the occurrence of a specific storm impact regime. Similarly, the elevation of the berm can determine the storm impact regime by allowing further incursions of the wave runup or halting the flow during moderate events. While in theory, a real-time simulation-based EWS would be more flexible to incorporate the variability of the pre-storm beach morphology and thus reduce some uncertainties of its predictions, in the practice, data acquisition, processing, and implementation in the numerical model made this objective highly complicated. Conversely, the incorporation of such data in a pre-computed EWS can be achieved by the simple addition of a new training data set covering different beach morphologies in a non-operational time window. This pre-computed information can be used for uncertainty analyses of a given event under different morphological conditions and for a better risk prediction of the impact of individual or consecutive storms. Hence, conditioning the EWS with specific initial morphologies can better represent the impact of consecutive storms.

According to the presented results, the uncertainty related to storm duration is generally lower than that associated with the pre-storm beach morphology for moderate events, such as 5- and 10-year events (up to 12% for proportional berm retreat and up to 4% for proportional dune retreat). Only when storm severity largely increases, the uncertainty related to storm duration becomes more relevant (41%) and the variability can go from relevant dune retreat to complete dune breaching, with different implications in terms of risk assessment. This would indicate that in a pre-computed EWS, the variable storm duration might not be essential to condition the prediction system and still obtain accurate beach erosion predictions for moderate events, but modelers should be aware of the limitations for very energetic events. Hence, the training data set supporting the pre-computed EWSs can be highly reduced. However, it is important to remark that when creating synthetic storms, the copula method or other statistical techniques must be employed to take into account the dependence between the different variables describing the storm and their natural variability. Furthermore, additional training by including extra events created with this methodology improves the capabilities of the prediction systems since more duration variability would be considered. For an EWS that uses as a proxy the relative eroded volume, the uncertainties related to storm duration would range between 10% and 20% approximately. Importantly, the uncertainties of both variables (duration and initial morphology) cannot be disconnected, and the storm duration variability can be enlarged depending on the pre-storm morphology. For instance, changes in dune erosion induced by storm duration variability are lower for beach profiles with high availability of sediment than for beach profiles that present a smaller amount of sediment. Therefore, if both variables are previously unknown in an EWS, the uncertainties in the relative eroded volume and the proportional dune retreat can be up to 30% and 60%, respectively, for extreme events, while the uncertainty in the proportional berm retreat can reach 90% for moderate events. To minimize these uncertainties, it is recommended that the EWS is built by including a comprehensive data set of existing morphologies, based on field surveys (preferably large datasets), and storm durations that are based on observations (e.g., buoys). That will enable a reduction of the expected variability for each coastal area and will limit the uncertainty.

While the sensitivity of other models to simulate storm-driven erosion and the beach-dune response to storm conditions has not been tested here, the obtained results serve to shed some light on the uncertainty of the

computed profile erosion and, they can be used to estimate the validity of assumptions when designing EWSs. One of the limitations of the pre-computed simulation-based EWSs is the schematization of real events using synthetic storms. Here, it was demonstrated that some simplifications such as the STSS can be applied, which can also be valid for other coastal areas. Hence, it is highly recommendable to investigate the validity of these simplifications when creating this type of EWS and apply statistical techniques (e.g., copula) for establishing relationships between the important variables (Poelhekke et al., 2016). If such relationships are not properly obtained and are not supported by measured data, it is probable that the simplified storms do not fully represent the real ones. Other aspects such as the impact of the tide conditions (spring vs. neap conditions) in the uncertainty analysis were not investigated since the variability observed with lower tidal ranges would be likely reduced and thus, less relevant for the uncertainty analysis when developing EWS. Finally, future studies might consider the application of the GLUE method (Simmons et al., 2017) to assess the inherent uncertainties of the modeling approach and their relative importance compared to other aspects involved in the development and implementation of an EWS.

5. Conclusions

Multiple one-dimensional XBeach simulations were performed to assess the uncertainty in the response of a steep beach-dune system to storm events with varying severity and duration, and pre-storm beach morphologies. The severity of the storm was defined based on different return periods (<1, 5, 10, 25, and 50 years) and the duration was established based on a linear adjustment with the $\langle H_{si} \rangle / \langle i \rangle$ (derived from field data) and the upper and lower confidence levels. The beach morphologies implemented in the model covered the natural variability of this demonstration site (from reflective to intermediate) reported by previous studies, with varying berm characteristics (height and width), and consequently subaerial beach volume, and submerged profile. Three morphological indicators were used: relative eroded volume, proportional berm retreat and proportional dune retreat. The results demonstrated that: (a) the uncertainty in the computed relative eroded volume due to the pre-storm beach morphology was low (maximum 8%), while the uncertainty related to storm duration was slightly higher (up to 18%), regardless of the storm severity. (b) The uncertainty in the proportional berm retreat due to the selection of the beach profile induced a large variability (up to 88%), especially for moderate events such as the 5- and 10-year events. The impact of storm duration variability on changes in this indicator was less important and it accounted for up to 12%. (c) The uncertainties in the proportional dune retreat due to initial morphology and storm duration increased with storm severity. The variability of the beach profile induced uncertainties between 14% and 41%, while the variability of the storm duration induced lower variations, between 2% and 40%. Moreover, for the most extreme event, when the longest duration was considered, dune breaching became a possible consequence. If the initial profile and storm duration were previously undetermined, then the uncertainty of the indicators increased. This uncertainty was very important in the proportional berm retreat for moderate events and the proportional dune retreat for very energetic events. In the future, with global predictions available for a longer lead time, the uncertainty related to defining the storm duration will be reduced. However, the developed methodology and findings of this study still contribute to determining the importance of including storm duration within the variables necessary to create the training information of a pre-computed EWS. Moreover, although these findings are primarily applicable to similar sites to the demonstration site (exposed steep beaches), the methodology developed here can be used in future studies as a benchmark test to assess and quantify the impact of these indicators in other coastal erosion prediction systems worldwide, with different beach morphologies (e.g., more dissipative) and wave climatologies.

Our results highlight that the pre-storm beach morphology and storm duration are very relevant aspects in determining the response of the coastal systems on steep beaches (beachface slope ~ 0.1 or larger), and consequently, the uncertainty associated with their variability should be evaluated when implementing an EWS devoted to coastal erosion. Also, the characteristics (location) of the coastal receptors affect the level of uncertainty of the EWS predictions. The knowledge generated here helps to quantify uncertainties and provides solid and scientific-based expertise that can be useful for the implementation of more reliable coastal erosion EWSs (real-time and pre-computed simulations) and subsequent risk reduction measures.

Conflict of Interest

The authors declare no conflicts of interest relevant to this study.

Data Availability Statement

Data that support the summary, results, tables, and figures of this study are available for downloading at J. L. Garzon et al. (2023, <https://doi.org/10.13140/RG.2.2.31149.36324>).

Acknowledgments

The authors acknowledge Fundação para a Ciência e Tecnologia (FCT), under the project LA/P/0069/2020 granted to the Associate Laboratory ARNET and UID/00350/2020 CIMA and the research project EW-COAST (ALG-LISBOA-01-145-FEDER-028657) attributed by the Foundation for Science and Technology, IP, supported by the Regional Operational Program of Algarve and the Regional Operational Program of Lisbon in its component FEDER and the Foundation for Science and Technology in its OE component. The authors also acknowledge the project LIFE18 NAT/PT/000927 – LIFE Ilhas Barreira “Conserving the Barrier Islands in Algarve to protect priority species and habitats”, funded by the LIFE EU programme. The authors would like also to acknowledge Professor Joaquim Luis for his active participation in processing and sharing bathymetric information (<http://w3.ualg.pt/~jluis/mirone/main.html>) and to Luísa Bon de Sousa for topographic data acquisition and processing. We also acknowledge the Instituto Hidrográfico and Puertos del Estado who supplied wave and water level data. COSMO Program (Programa de Monitorização da Faixa Costeira de Portugal Continental) of Agência Portuguesa do Ambiente, co-funded by the Programa Operacional Sustentabilidade e Eficiência no Uso de Recursos (POSEUR), is also acknowledged for data availability (<https://cosmo.apambiente.pt>). Theocharis Plomaritis has been also co-financed by the 2014–2020 ERDF Operational Programme and by the Department of Economy, Knowledge, Business and University of the Regional Government of Andalusia. Project reference: FEDER-UCA18-107062 and the Spanish national funded project CRISIS, Project reference: PID2019-109143RB-I00.

References

- Adapt Now: A Global Call for Leadership on Climate Resilience. (2019). <https://doi.org/10.1596/32362>
- Almeida, L. P. (2007). *Variabilidade do Perfil de Praia em Função da Agitação Marítima. Projecto Técnico-científico da Licenciatura em Oceanografia*. Universidade do Algarve, Faculdade de Ciências e do Ambiente.
- Almeida, L. P., Ferreira, Ó., & Pacheco, A. (2011a). Thresholds for morphological changes on an exposed sandy beach as a function of wave height. *Earth Surface Processes and Landforms*, 36(4), 523–532. <https://doi.org/10.1002/esp.2072>
- Almeida, L. P., Ferreira, Ó., & Taborada, R. (2011b). Geoprocessing tool to model beach erosion due to storms: Application to Faro beach (Portugal). *Journal of Coastal Research*, 64, 1830–1834.
- Almeida, L. P., Voussdoukas, M. V., Ferreira, Ó., Rodrigues, B. A., & Matias, A. (2012). Thresholds for storm impacts on an exposed sandy coastal area in southern Portugal. *Geomorphology*, 143–144, 3–12. <https://doi.org/10.1016/j.geomorph.2011.04.047>
- Amores, A., Marcos, M., Carrió, D. S., & Gomez-Pujol, L. (2020). Coastal impacts of Storm Gloria (January 2020) over the north-western Mediterranean. *Natural Hazards and Earth System Sciences*, 20(7), 1955–1968. <https://doi.org/10.5194/nhess-20-1955-2020>
- Anfuso, G., & Ruiz, N. (2004). Morfodinámica de una playa mesomareal expuesta con terraza de bejamar (Faro, Sur de Portugal). *Ciencias Marinas*, 30(4), 575–584. <https://doi.org/10.7773/cm.v30i4.341>
- Armaroli, C., Grottolli, E., Harley, M. D., & Ciavola, P. (2013). Beach morphodynamics and types of foredune erosion generated by storms along the Emilia-Romagna coastline, Italy. *Geomorphology*, 199, 22–35. <https://doi.org/10.1016/j.geomorph.2013.04.034>
- Arnoux, F., Abadie, S., Bertin, X., & Kojadinovic, I. (2021). Coastal flooding event definition based on damages: Case study of Biarritz Grande Plage on the French Basque coast. *Coastal Engineering*, 166, 135907. <https://doi.org/10.1016/j.coastaleng.2021.103873>
- Balouin, Y., Howa, H., & Rafecas, N. (2000). Morphodynamique de croissants de plage, Plage de Faro, Sud Portugal. In *7th Colloque de l'Union des Océanographes Français, La Rochelle, France*.
- Barnard, P. L., van Ormondt, M., Erikson, L. H., Eshleman, J., Hapke, C., Ruggiero, P., et al. (2014). Development of the Coastal Storm Modeling System (CoSMoS) for predicting the impact of storms on high-energy, active-margin coasts. *Natural Hazards*, 74(2), 1095–1125. <https://doi.org/10.1007/s11069-014-1236-y>
- Beuzen, T., Harley, M. D., Splinter, K. D., & Turner, I. L. (2019). Controls of variability in berm and dune storm erosion. *Journal of Geophysical Research: Earth Surface*, 124(11), 2647–2665. <https://doi.org/10.1029/2019JF005184>
- Booi, N., Ris, R. C., & Holthuijsen, L. H. (1999). A third-generation wave model for coastal regions: 1. Model description and validation. *Journal of Geophysical Research*, 104(C4), 7649–7666. <https://doi.org/10.1029/98JC02622>
- Callaghan, D. P., Nielsen, P., Short, A., & Ranasinghe, R. (2008). Statistical simulation of wave climate and extreme beach erosion. *Coastal Engineering*, 55(5), 375–390. <https://doi.org/10.1016/j.coastaleng.2007.12.003>
- Callaghan, D. P., Ranasinghe, R., & Roelvink, D. (2013). Probabilistic estimation of storm erosion using analytical, semi-empirical, and process based storm erosion models. *Coastal Engineering*, 82, 64–75. <https://doi.org/10.1016/j.coastaleng.2013.08.007>
- Castelle, B., Marieu, V., Bujan, S., Splinter, K. D., Robinet, A., Sénéchal, N., & Ferreira, S. (2015). Impact of the winter 2013–2014 series of severe Western Europe storms on a double-barred sandy coast: Beach and dune erosion and megacusp embayments. *Geomorphology*, 238, 135–148. <https://doi.org/10.1016/j.geomorph.2015.03.006>
- Cho, M., Yoon, H.-D., Yang, J.-A., & Son, S. (2019). Sensitivity and uncertainty analysis of coastal numerical model under various beach conditions in Korea. In *Proceedings of the 9th International Conference* (pp. 481–487). Coastal Sediment.
- Ciavola, P., Ferreira, Ó., Van Dongeren, A., Van Thiel de Vries, J., Armaroli, C., & Harley, M. (2014). Prediction of storm impacts on beach and dune systems. *Hydrometeorological Hazards: Interfacing Science and Policy*, 9781118629, 227–252. <https://doi.org/10.1002/9781118629567.ch3d>
- Ciavola, P., Taborada, R., Ferreira, Ó., & Dias, J. A. (1997). Field observations of sand-mixing depths on steep beaches. *Marine Geology*, 141(1–4), 147–156. [https://doi.org/10.1016/S0025-3227\(97\)00054-6](https://doi.org/10.1016/S0025-3227(97)00054-6)
- Cohn, N., Ruggiero, P., Garcia-Medina, G., Anderson, D., Serafin, K. A., & Biel, R. (2019). Environmental and morphologic controls on wave-induced dune response. *Geomorphology*, 329, 108–128. <https://doi.org/10.1016/j.geomorph.2018.12.023>
- Costa, M., Silva, R., & Vitorino, J. (2001). Contribuição para o Estudo do Clima de Agitação Marítima na Costa Portuguesa. In *II Jornadas Portuguesas de Engenharia Costeira e Portuária*.
- Crapoulet, A., Héquette, A., Marin, D., Levoy, F., & Patrice, B. (2017). Variations in the response of the dune coast of northern France to major storms as a function of available beach sediment volume. *Earth Surface Processes and Landforms*, 27(January), 1603–1622. <https://doi.org/10.1002/esp.4098>
- Davies, G., Callaghan, D. P., Gravios, U., Jiang, W., Hanslow, D., Nichol, S., & Baldock, T. (2017). Improved treatment of non-stationary conditions and uncertainties in probabilistic models of storm wave climate. *Coastal Engineering*, 127(June), 1–19. <https://doi.org/10.1016/j.coastaleng.2017.06.005>
- Do, K., Shin, S., Cox, D., & Yoo, J. (2018). Numerical simulation and large-scale physical modelling of coastal sand dune erosion. *Journal of Coastal Research*, 85, 196–200. <https://doi.org/10.2112/S185-040.1>
- Duo, E., Sanuy, M., Jiménez, J. A., & Ciavola, P. (2020). How good are symmetric triangular synthetic storms to represent real events for coastal hazard modelling. *Coastal Engineering*, 159(August 2019), 103728. <https://doi.org/10.1016/j.coastaleng.2020.103728>
- Eichentopf, S., Karunarathna, H., & Alsina, J. M. (2019). Morphodynamics of sandy beaches under the influence of storm sequences: Current research status and future needs. *Water Science and Engineering*, 12(3), 221–234. <https://doi.org/10.1016/j.wse.2019.09.007>
- Fairley, I., Horrillo-caraballo, J., Masters, I., Karunarathna, H., & Reeve, D. E. (2020). Spatial variation in coastal dune evolution in a high tidal range environment. *Remote Sensing*, 20(22), 3689. <https://doi.org/10.3390/rs12223689>
- Ferreira, Ó. (2005). Storm groups versus extreme single storms: Predicted erosion and management consequences. *Journal of Coastal Research*, SI(42), 221–227.
- Ferreira, Ó., Garcia, T., Matias, A., Taborada, R., & Dias, J. A. (2006). An integrated method for the determination of set-back lines for coastal erosion hazards on sandy shores. *Continental Shelf Research*, 26(9), 1030–1044. <https://doi.org/10.1016/j.csr.2005.12.016>
- Ferreira, Ó., Martins, J. T., & Dias, J. A. (1997). *Morfodinâmica e vulnerabilidade da Praia de Faro. Livro de Comunicações Do Seminário Sobre a Zona Costeira Do Algarve* (pp. 67–76). EUROCOAST Portugal.

- Ferreira, Ó., Matias, A., & Pacheco, A. (2016). The East Coast of Algarve: A barrier island dominated coast. *Thalassas: International Journal of Marine Science*, 32(2), 75–85. <https://doi.org/10.1007/s41208-016-0010-1>
- Ferreira, Ó., Plomaritis, T. A., & Costas, S. (2017). Process-based indicators to assess storm induced coastal hazards. *Earth-Science Reviews*, 173(August), 159–167. <https://doi.org/10.1016/j.earscirev.2017.07.010>
- Ferreira, Ó., Plomaritis, T. A., & Costas, S. (2019). Effectiveness assessment of risk reduction measures at coastal areas using a decision support system: Findings from Emma storm. *Science of the Total Environment*, 657, 124–135. <https://doi.org/10.1016/j.scitotenv.2018.11.478>
- Ferreira, Ó., Taborda, R., & Dias, J. A. (1998). Morphological vulnerability index: A simple way of determining beach behaviour. *Coastal Engineering*, 3206–3214. <https://doi.org/10.1061/9780784404119.243>
- Ferreira, Ó., Viavattene, C., Jim, J. A., Bolle, A., Neves, L., Plomaritis, T. A., et al. (2018). Storm-induced risk assessment: Evaluation of two tools at the regional and hotspot scale. *Coastal Engineering*, 134(September 2017), 241–253. <https://doi.org/10.1016/j.coastaleng.2017.10.005>
- Fortunato, A. B., Li, K., Bertin, X., Rodrigues, M., & Miguez, B. M. (2016). Determination of extreme sea levels along the Iberian Atlantic coast. *Ocean Engineering*, 111, 471–482. <https://doi.org/10.1016/j.oceaneng.2015.11.031>
- Garzon, J. L., Ferreira, A., Ferreira, Ó., Fortes, C., & Reis, M. (2020). Beach State Report: Quarteira, Praia de Faro and Costa da Caparica. Retrieved from https://www.cima.ualg.pt/ew-coast/wp-content/uploads/2020/09/Beach_state_report-.pdf
- Garzon, J. L., Costas, S., & Ferreira, Ó. (2022). Biotic and abiotic factors governing dune response to storm events. *Earth Surface Processes and Landforms*, 47(4), 1013–1031. <https://doi.org/10.1002/esp.5300>
- Garzon, J. L., Ferreira, Ó., & Plomaritis, T. A. (2022a). Modeling of coastal erosion in exposed and groin-protected steep. *Journal of Waterway, Port, Coastal, and Ocean Engineering*, 148(6), 1–26. [https://doi.org/10.1061/\(ASCE\)WW.1943-5460.0000719](https://doi.org/10.1061/(ASCE)WW.1943-5460.0000719)
- Garzon, J. L., Ferreira, Ó., & Plomaritis, T. A. (2022b). Modelling storm-driven erosion in natural and protected steep beaches. In *Proceedings of the 39th IAHR World Congress* (pp. 5764–5770).
- Garzon, J. L., Plomaritis, T. A., & Ferreira, O. (2023). Uncertainty analysis related to beach morphology and storm duration for more reliable early warning systems for coastal hazards [Dataset]. ResearchGate. <https://doi.org/10.13140/RG.2.2.31149.36324>
- Guisado-Pintado, E., & Jackson, D. W. T. (2018). Multi-scale variability of storm Ophelia 2017: The importance of synchronised environmental variables in coastal impact. *Science of the Total Environment*, 630, 287–301. <https://doi.org/10.1016/j.scitotenv.2018.02.188>
- Haerens, P. (2009). *Seasonal and storm induced morphological variations at Praia de Faro, Península do Anção*. Southern Portugal.
- Harley, M. D., Turner, I. L., Kinsela, M. A., Middleton, J. H., Mumford, P. J., Splinter, K. D., et al. (2017). Extreme coastal erosion enhanced by anomalous extratropical storm wave direction. *Scientific Reports*, 7(1), 1–9. <https://doi.org/10.1038/s41598-017-05792-1>
- Harley, M. D., Turner, I. L., Splinter, K. D., Phillips, M. S., & Simmons, J. A. (2016). Beach response to Australian East Coast lows: A comparison between the 2007 and 2015 events, Narrabeen-Collaroy Beach. *Journal of Coastal Research*, 1(75), 388–392. <https://doi.org/10.2112/S175-078.1>
- Harley, M. D., Valentini, A., Armaroli, C., Perini, L., Calabrese, L., & Ciavola, P. (2016). Can an early-warning system help minimize the impacts of coastal storms? A case study of the 2012 Halloween storm, northern Italy. *Natural Hazards and Earth System Sciences*, 16(1), 209–222. <https://doi.org/10.5194/nhess-16-209-2016>
- Jäger, W. S., Christie, E. K., Hanea, A. M., den Heijer, C., & Spencer, T. (2018). A Bayesian network approach for coastal risk analysis and decision making. *Coastal Engineering*, 134(May 2017), 48–61. <https://doi.org/10.1016/j.coastaleng.2017.05.004>
- Kalligeris, N., Smit, P. B., Ludka, B. C., Guza, R. T., & Gallien, T. W. (2020). Calibration and assessment of process-based numerical models for beach profile evolution in southern California. *Coastal Engineering*, 158(January), 103650. <https://doi.org/10.1016/j.coastaleng.2020.103650>
- Kriebel, D. L., & Dean, R. G. (1993). Convolution method for time-Dependent beach-profile response. *Journal of Waterway, Port, Coastal and Ocean Engineering*, ASCE, 119(2), 204–226. [https://doi.org/10.1061/\(asce\)0733-950x\(1993\)119:2\(204\)](https://doi.org/10.1061/(asce)0733-950x(1993)119:2(204))
- Lavell, A., Oppenheimer, M., Diop, C., Hess, J., Lempert, R., Li, J., et al. (2012). Climate change: New dimensions in disaster risk, exposure, vulnerability, and resilience. In *Managing the risks of extreme events and disasters to advance climate change adaptation: Special report of the intergovernmental panel on climate change* (p. 9781107025). <https://doi.org/10.1017/CBO9781139177245.004>
- Lerma, A. N., Bulteau, T., Muller, H., Decarsin, C., Gillet, R., Paris, F., et al. (2018). Towards the development of a storm erosion EWS for the French Aquitaine Coast. *Journal of Coastal Research*, 85(May), 666–670. <https://doi.org/10.2112/SI85-134.1>
- Luijendijk, A., Hagenaars, G., Ranasinghe, R., Baart, F., Donchyt, G., & Aarninkhof, S. (2018). The state of the world's beaches. *Scientific Reports*, 8(1), 1–11. <https://doi.org/10.1038/s41598-018-24630-6>
- Luis, J. F. (2007). Mirone: A multi-purpose tool for exploring grid data. *Computers & Geosciences*, 33(1), 31–41. <https://doi.org/10.1016/j.cageo.2006.05.005>
- Malvarez, G., Ferreira, Ó., Navas, F., Cooper, J. A. G., Gracia-Prieto, F. J., & Talavera, L. (2021). Storm impacts on a coupled human-natural coastal system: Resilience of developed coasts. *Science of the Total Environment*, 768, 144987. <https://doi.org/10.1016/j.scitotenv.2021.144987>
- Mangor, K., Drønen, N. K., Kærgaard, K. H., & Kristensen, S. E. (2017). *Shoreline management guidelines*. DHI Water and Environment.
- Martins, J., Tomé-Ferreira, Ó., Ciavola, P., & Dias, J. A. (1996). Monitoring of profile changes at Praia de Faro (Algarve): A tool to predict and solve problems. In *Partnership in coastal zone management* (pp. 615–622). Samara Publishing.
- Martins, J. T., Ferreira, Ó., & Dias, J. A. (1997). *A susceptibilidade da Praia de Faro à erosão por tempestades* (pp. 206–213). 9º Congresso Do Algarve.
- Masselink, G., & Short, A. D. (1993). The effect of tide range on beach morphodynamics and morphology: A conceptual beach model. *Journal of Coastal Research*.
- McCall, R. T., de Vries, J. S. M. V. T., Plant, N. G., Dongeren, A. R. V., Roelvink, J. A., Thompson, D. M., & Reniers, A. J. H. M. (2010). Two-dimensional time dependent hurricane overwash and erosion modeling at Santa Rosa Island. *Coastal Engineering*, 57(7), 668–683. <https://doi.org/10.1016/j.coastaleng.2010.02.006>
- Mendoza, E. T., Jimenez, J. A., & Mateo, J. (2011). A coastal storms intensity scale for the Catalan sea (NW Mediterranean). *Natural Hazards and Earth System Sciences*, 11(9), 2453–2462. <https://doi.org/10.5194/nhess-11-2453-2011>
- Mentaschi, L., Vousdoukas, M. I., Pekel, J. F., Voukouvalas, E., & Feyen, L. (2018). Global long-term observations of coastal erosion and accretion. *Scientific Reports*, 8(1), 1–11. <https://doi.org/10.1038/s41598-018-30904-w>
- Mickey, R. C., Dalyander, P. S., McCall, R., & Passeri, D. L. (2020). Sensitivity of storm response to antecedent topography in the XBeach model.
- Pires, H. O. (1998). *Project INDIA. Preliminary report on wave climate at Faro*. Instituto de Meteorologia.
- Plomaritis, T. A., Costas, S., & Ferreira, Ó. (2018). Use of a Bayesian Network for coastal hazards, impact and disaster risk. *Coastal Engineering*, 134(February 2017), 134–147. <https://doi.org/10.1016/j.coastaleng.2017.07.003>
- Plomaritis, T. A., Ferreira, Ó., Costas, S., & Puig, M. (2019). Storm induced coastal erosion: Indicators selection and comparison of three modelling approaches. In *X Jornadas de Geomorfología Litoral* (pp. 37–40).
- Poelhekke, L., Jäger, W. S., van Dongeren, A., Plomaritis, T. A., McCall, R., & Ferreira, Ó. (2016). Predicting coastal hazards for sandy coasts with a Bayesian Network. *Coastal Engineering*, 118, 21–34. <https://doi.org/10.1016/j.coastaleng.2016.08.011>

- PROGRAMA COSMO. (2018). Retrieved from <https://cosmo.apambiente.pt>
- Rafati, Y., Hsu, T. J., Elgar, S., Raubenheimer, B., Quataert, E., & van Dongeren, A. (2021). Modeling the hydrodynamics and morphodynamics of sandbar migration events. *Coastal Engineering*, *166*(February), 103885. <https://doi.org/10.1016/j.coastaleng.2021.103885>
- Ranasinghe, R. (2016). Assessing climate change impacts on open sandy coasts: A review. *Earth-Science Reviews*, *160*, 320–332. <https://doi.org/10.1016/j.earscirev.2016.07.011>
- Rodrigues, B. A., Matias, A., & Ferreira, Ó. (2012). Overwash hazard assessment. *Geológica Acta*, *10*(4), 427–437. <https://doi.org/10.1344/105.000001743>
- Roelvink, D., Reniers, A., van Dongeren, A., vande Thiel Vries, J., McCall, R., & Lescinski, J. (2009). Modelling storm impacts on beaches, dunes and barrier islands. *Coastal Engineering*, *56*(11–12), 1133–1152. <https://doi.org/10.1016/j.coastaleng.2009.08.006>
- Sallenger, A. H. (2000). Storm impact scale for barrier islands. *Journal of Coastal Research*, *16*(3), 890–895. <http://www.jstor.org/stable/4300099>
- Sánchez-Arcilla, A., Mendoza, E. T., Jiménez, J. A., Peña, C., Galofré, J., & Novoa, M. (2009). Beach erosion and storm parameters: Uncertainties for the Spanish Mediterranean. *Coastal Engineering*, *2008*, 2352–2362. https://doi.org/10.1142/9789814277426_0194
- Santos, V. M., Wahl, T., Long, J. W., Passeri, D. L., & Plant, N. G. (2019). Combining numerical and statistical models to predict storm-induced dune erosion. *Journal of Geophysical Research: Earth Surface*, *124*(7), 1817–1834. <https://doi.org/10.1029/2019JF005016>
- Sanuy, M., Duo, E., Jäger, W. S., Ciavola, P., & Jiménez, J. A. (2018). Linking source with consequences of coastal storm impacts for climate change and risk reduction scenarios for Mediterranean sandy beaches. *Natural Hazards and Earth System Sciences*, *18*(7), 1825–1847. <https://doi.org/10.5194/nhess-18-1825-2018>
- Sá-Pires, A. C., Taborda, R., Ferreira, Ó., Dias, J. A., & Grande, C. (2006). Beach volume changes: Vertical datum definition. *Journal of Coastal Research*, *39*(1), 341–344.
- Scott, T., Masselink, G., O'Hare, T., Saulter, A., Poate, T., Russell, P., et al. (2016). The extreme 2013/2014 winter storms: Beach recovery along the southwest coast of England. *Marine Geology*, *382*, 224–241. <https://doi.org/10.1016/j.margeo.2016.10.011>
- Seok, J. S., & Suh, S. W. (2018). Efficient real-time erosion early warning system and artificial sand dune breaching on Haeundae Beach, Korea. *Journal of Coastal Research*, *85*, 186–190. <https://doi.org/10.2112/S185-038.1>
- Simmons, J. A., Harley, M. D., Marshall, L. A., Turner, I. L., Splinter, K. D., & Cox, R. J. (2017). Calibrating and assessing uncertainty in coastal numerical models. *Coastal Engineering*, *125*(April), 28–41. <https://doi.org/10.1016/j.coastaleng.2017.04.005>
- Simmons, J. A., Splinter, K. D., Harley, M. D., & Turner, I. L. (2019). Calibration data requirements for modelling subaerial beach storm erosion. *Coastal Engineering*, *152*(November 2018), 103507. <https://doi.org/10.1016/j.coastaleng.2019.103507>
- Smallegan, S. M., Irish, J. L., Van Dongeren, A. R., & Den Bieman, J. P. (2016). Morphological response of a sandy barrier island with a buried seawall during Hurricane Sandy. *Coastal Engineering*, *110*, 102–110. <https://doi.org/10.1016/j.coastaleng.2016.01.005>
- Splinter, K. D., Carley, J. T., Golshani, A., & Tomlinson, R. (2014). A relationship to describe the cumulative impact of storm clusters on beach erosion. *Coastal Engineering*, *83*, 49–55. <https://doi.org/10.1016/j.coastaleng.2013.10.001>
- Splinter, K. D., Kearney, E. T., & Turner, I. L. (2018). Drivers of alongshore variable dune erosion during a storm event: Observations and modelling. *Coastal Engineering*, *131*, 31–41. <https://doi.org/10.1016/j.coastaleng.2017.10.011>
- Splinter, K. D., & Palmsten, M. L. (2012). Modeling dune response to an East Coast Low. *Marine Geology*, *329–331*, 46–57. <https://doi.org/10.1016/j.margeo.2012.09.005>
- Stockdon, H. F., Holman, R. A., Howd, P. A., & Sallenger, A. H. (2006). Empirical parameterization of setup, swash, and runup. *Coastal Engineering*, *53*(7), 573–588. <https://doi.org/10.1016/j.coastaleng.2005.12.005>
- Suzuki, T., & Cox, D. T. (2021). Evaluating XBeach performance for extreme offshore-directed sediment transport events on a dissipative beach. *Coastal Engineering Journal*, *00*(00), 1–15. <https://doi.org/10.1080/21664250.2021.1976452>
- Valchev, N., Andreeva, N., Eftimova, P., & Trifonova, E. (2014). Prototype of early warning system for coastal storm hazard (Bulgarian black sea coast). *Comptes Rendus de L'Academie Bulgare Des Sciences*, *67*(7), 971–978.
- Valchev, N., Eftimova, P., & Andreeva, N. (2016). Implementation and validation of a multi-domain coastal hazard forecasting system in an open bay. *Coastal Engineering*, *134*, 1–17. <https://doi.org/10.1016/j.coastaleng.2017.08.008>
- van Bemmelen, C. W. T., de Schipper, M. A., Darnall, J., & Aarninkhof, S. G. J. (2020). Beach scarp dynamics at nourished beaches. *Coastal Engineering*, *160*(July 2019), 103725. <https://doi.org/10.1016/j.coastaleng.2020.103725>
- Van Dongeren, A., Ciavola, P., Viavattene, C., De Kleermaeker, S., Martinez, G., Ferreira, O., et al. (2014). RISC-KIT: Resilience-increasing strategies for coasts - ToolKIT. *Journal of Coastal Research*, *70*, 366–371. <https://doi.org/10.2112/S170-062.1>
- Vousdoukas, M. I. (2012). Erosion/accretion patterns and multiple beach cusp systems on a meso-tidal, steeply-sloping beach. *Geomorphology*, *141–142*, 34–46. <https://doi.org/10.1016/j.geomorph.2011.12.003>
- Vousdoukas, M. I., Almeida, L. P. M., & Ferreira, Ó. (2012). Beach erosion and recovery during consecutive storms at a steep-sloping, meso-tidal beach. *Earth Surface Processes and Landforms*, *37*(6), 583–593. <https://doi.org/10.1002/esp.2264>
- Vousdoukas, M. I., Ferreira, Ó., Almeida, L. P., & Pacheco, A. (2012). Toward reliable storm-hazard forecasts: XBeach calibration and its potential application in an operational early-warning system. *Ocean Dynamics*, *62*(7), 1001–1015. <https://doi.org/10.1007/s10236-012-0544-6>
- Vousdoukas, M. I., Ioannis, M., Wziatek, D., & Almeida, L. P. (2012). Coastal vulnerability assessment based on video wave run-up observations at a mesotidal, steep-sloped beach. *Ocean Dynamics*, *62*(1), 123–137. <https://doi.org/10.1007/s10236-011-0480-x>
- Vousdoukas, M. I., Ranasinghe, R., Mentaschi, L., Plomaritis, T. A., Athanasiou, P., Luijendijk, A., & Feyen, L. (2020). Sandy coastlines under threat of erosion. *Nature Climate Change*, *10*(3), 260–263. in press. <https://doi.org/10.1038/s41558-020-0697-0>

Erratum

Since the original publication of this article the first two sentences of the acknowledgments section have been revised to include additional funding information from Fundação para a Ciência e Tecnologia and the LIFE EU programme. This may be considered the authoritative version of record.